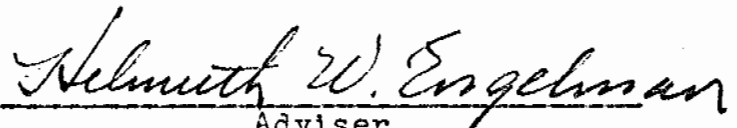


NON-MECHANICAL SUPERCHARGING OF A
FOUR-STROKE DIESEL ENGINE

A Thesis
Presented in Partial Fulfillment
of the Requirements for the
Degree Master of Science

By
MICHAEL PAUL THOMPSON, B.M.E.
The Ohio State University
1968

Approved by:


Adviser
Department of Mechanical Engineering

The University assumes no responsibility
for the accuracy or correctness of any of the
statements or opinions expressed in this thesis.

ACKNOWLEDGEMENTS

The author wishes to express appreciation to Professor H. W. Engelman, of the Department of Mechanical Engineering of the Ohio State University, for his aid and guidance during the completion of the experimentation and the development of this thesis; to Cummins Diesel for providing the engine and some of the equipment used in the experiments and testing; and to Mr. Long, Mr. Mosley and Mr. Sweet, of the Robinson Laboratory shop staff for their cooperation and aid during the experimentation. Appreciation is also extended to the author's wife, Marilyn, for typing the manuscript and for giving encouragement during the development of this thesis.

TABLE OF CONTENTS

	Page
STATEMENT OF THE PROBLEM	v
CHAPTER I	
INTRODUCTION AND HISTORY	1
APPROACH INVESTIGATED	5
CHAPTER II	
ENGINE AND EQUIPMENT	11
CHAPTER III	
LINEARITY AND REPEATABILITY OF PRESSURE MEASURED	13
NEEDED ADDITIONAL CALCULATIONS AND RESULTS	19
CHAPTER IV	
OTHER DATA	24
TEST RESULTS	30
CHAPTER V	
CONCLUSIONS	35
BIBLIOGRAPHY	37
APPENDIX	
TABLE 1	41
TABLE 2	42
TABLE 3	43
TABLE 4	44
TABLE 5	45
TABLE 6	46
FIGURES 8 through 24	49 - 65

STATEMENT OF THE PROBLEM

The purpose of this thesis was to investigate the most significant phenomena involved in increasing the breathing of a naturally aspirated four-stroke diesel engine with individual inlet pipes.

CHAPTER I

INTRODUCTION AND HISTORY

That the volumetric efficiency of a single cylinder non-supercharged four-stroke engine can be changed significantly through alterations in the design of the induction system is well known. The design criterion which should be used to obtain a high volumetric efficiency is not, however, generally agreed upon. Historically there have been two approaches which have been frequently used to investigate increasing volumetric efficiency of an engine. The term "engine" will henceforth be used to mean single cylinder non-supercharged four-stroke engine. It must be noted that, as a basis for design, both of these approaches have serious shortcomings.

The simplest approach investigates the vibrations of the gas in the inlet pipe alone.

Various authors have used this approach:*

Morse, Boden & Schechter⁽⁶⁾, Lutz⁽⁷⁾, Boden & Schechter⁽⁸⁾, Kastner⁽⁹⁾, Binder & Hall⁽¹⁰⁾,

*(N, p. M) refers to item number (N) in the bibliography and the specific page (M) of that item when appropriate.

Lichty⁽¹¹⁾, Platner⁽¹²⁾, Platner⁽¹⁴⁾, McMunn,
Yoerger & Weber⁽¹⁶⁾, Geschelin⁽¹⁸⁾, Lichty⁽¹⁹⁾.

This approach attempts to amplify and utilize the pressure waves which are set up in the inlet pipe as a result of the flow interruption when the inlet valve closes. If the pressure wave oscillates slightly more than an integer number of times while one engine cycle is completed, the pressure wave should be amplified and aid the next induction process. The period in seconds of the inlet pipe with the valve closed is $4L/12c = L/3c$, where L is the length of the intake to the inlet valve in inches and c is the speed of sound in feet per second. Thus the period of the engine divided by the period of the pipe should be roughly an integer, N , equal to 3, 4 or 5^(6, p.19). In equation form we get

$$\frac{120}{\text{RPM}} \times \frac{3c}{L} = \frac{360c}{\text{RPM} \times L} = N$$

Thus the required pipe length is $L = \frac{360c}{N \times \text{RPM}}$.

Though this approach has the desirable quality of simplicity it has several serious shortcomings. It does not take cylinder size and inlet pipe area into account. It does not account for the increase in volumetric efficiency

(over no inlet pipe) when N is not near an integer. Although the phenomenon described by this approach does have a significant effect upon volumetric efficiency, it does not appear to be the most significant phenomenon involved since the "available data seem to indicate that the difference in power output due to resonance (of the inlet pipe as an organ pipe), or lack of it, is often small compared to the difference in power output with or without the use of an inlet pipe." (13, p.1133)

The more involved approach is based upon an analysis of the induction process itself. Since various authors, List⁽⁴⁾, Dennison⁽⁵⁾, Taylor, Livengood & Tsai⁽¹³⁾, have used different specific assumptions the thermodynamic and physical systems modeled have varied; but this does not effect the general approach used. Once sufficient assumptions have been made a differential equation or set of equations describing the induction process can be obtained. Since the equation or set of equations thus obtained have not in the past been solvable in closed form, approximate or numerical techniques had to be used. Often dimensionless or grouped parameters are defined to facilitate working with the equation or set of equations.

The result of this type of approach is plots of cylinder pressure or volumetric efficiency versus crank angle for various values of the various parameters chosen. Although this type of approach gives adequate results as far as predicting the shape of the volumetric efficiency versus RPM curve, it is not a convenient design tool in that one can not obtain directly the manifold dimensions needed to give the desired shape performance curve. Also, this approach does not attempt to describe the basic phenomena by which an increase in volumetric efficiency is obtained through proper manifold design.

APPROACH INVESTIGATED

The approach investigated in this thesis was formulated by H. W. Engelman⁽²⁰⁾. For this approach the engine during the induction process is modeled as a Helmholtz resonator with a modulated volume, see Figure 1.

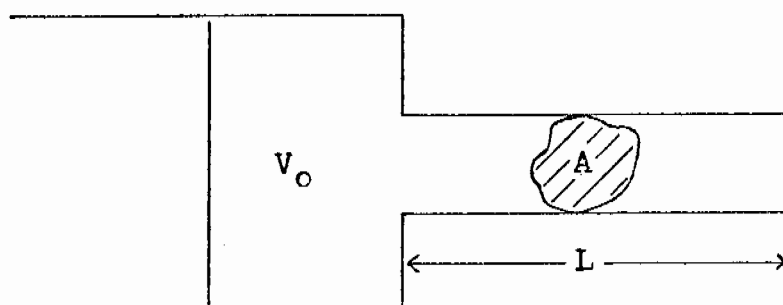


Figure 1

where A area, square inches
 L length, inches
 V_o cylinder volume at midstroke,
 cubic inches

Engelman states that to best utilize the momentum of the gases in the inlet pipe the induction system (Helmholtz resonator with modulated volume) should go through one resonant oscillation during one induction period.^(20, p.48) Thus the Helmholtz type oscillation is initiated and utilized during one induction process. Organ-pipe type oscillations

initiated by the Helmholtz oscillation may have an effect upon the next induction process if they are of sufficient magnitude and phased properly; but as stated before, the organ pipe type resonance is not the most significant influencing factor on engine breathing. The fact that each Helmholtz type oscillation is initiated and utilized during one induction process gives rise to two differences between Helmholtz type resonance and organ pipe type resonance.

1. With Helmholtz type resonance each induction process is isolated from every other induction process. Thus the relationship between Helmholtz frequency and engine frequency is not necessarily expected to be an integer.
2. The speed range over which an increase in breathing occurs is much larger for the Helmholtz type resonance. This is a result of the fact that: the pressure rise which is to be utilized exists for a much longer period of time (relative to the period of the induction process) for the Helmholtz type resonance.

The natural frequency of a Helmholtz resonator with a fixed volume is well known and can be

obtained in almost any acoustics text such as Wood⁽²¹⁾.

$$f = \frac{c}{2\pi} \sqrt{\frac{S}{LV_c}}$$

where f frequency, cycles per second
 c speed of sound in air, inches
 per second
 S area of pipe, square inches
 L length of pipe, inches
 V_c volume of chamber, cubic inches

Defining the mean static natural frequency of the engine as its natural frequency when the piston is at midstroke, as Engelman did, we get:

$$f_s = \frac{360\sqrt{2}}{\pi} c \sqrt{\frac{A}{L_e V}} \sqrt{\frac{R-1}{R+1}}$$

where f_s mean static natural frequency,
 cycles per minute
 c speed of sound, feet per second
 A area of inlet pipe, square inches
 L_e the effective length of inlet
 pipe, inches
 V displacement volume of the engine,
 cubic inches
 R compression ratio

Since the volume at midstroke equals $\frac{V}{2}$ plus V_{cl} , where V_{cl} is the clearance volume and is related to the displacement volume and compression ratio by V_{cl} equals $\frac{V}{R-1}$ thus:

$$V_c = \frac{V}{2} \times \frac{(R-1)}{(R-1)} + \frac{2V}{2(R-1)} = \frac{V}{2} \times \frac{R+1}{R-1}$$

The effect the changing volume has on the system natural frequency has been investigated in Engelman's dissertation. The assumptions used in his analysis are that:

- a) heat transfer and friction are negligible,
- b) the gas in the inlet pipe is incompressible,
- c) and the gas in the chamber acts as a linear spring.

The resulting differential equation is a form of Hill's equation, and Engelman utilized Cambi's paper⁽²²⁾ to obtain the system natural frequency. The conclusion of this analysis is that the changing chamber volume does have an effect upon the natural frequency of the system, but that this effect is small enough so that the true natural frequency can be approximated by the mean static natural frequency as defined above.

As stated above the induction system period should be approximately equal to the period of the

induction process. The period of the induction process is equal to $1/(a \times \text{RPM})$ where "a" is on the order of 2 for most conventional engines but does vary depending upon inlet port and inlet valve geometry and valve timing. The induction system period is equal to $1/(b \times f_s)$ where "b" is approximately 1. It should be noted that b "depends more upon the amount of modulation than upon the modulating frequency." (20, p.40) Solving for the RPM at which optimum performance should be obtained, we get:

$$\text{RPM} = \frac{1}{k} f_s = \frac{162}{k} c \sqrt{\frac{A}{L_e V}} \sqrt{\frac{R-1}{R+1}}$$

where k is approximately 2 and more dependent upon engine characteristics than operating conditions. The other symbols are defined on page 7.

This thesis will investigate the correlation of the approach just outlined to experimental results. In the experimental work done various inlet geometries were investigated. Not only were the effects of different length pipes and different area pipes investigated, but also the effects of curved pipes, pipes with and without well-rounded entrances, non-circular tubes and pipes of non-constant area. Analytically considering inlet tubes of different length, area and shape

requires no modification of the above equation.

The pipes of non-constant area, however, require a method for computing an effective A/L . In reference to this problem Wood⁽²¹⁾ states that:

$$\frac{L}{A}|_{\text{effective}} = \int_0^L \frac{dx}{A} = \sum_{i=1}^{\text{number of sections}} \frac{L_i}{A_i}.$$

CHAPTER II

ENGINE AND EQUIPMENT

The engine used for the tests was a Cummins V-6 diesel engine, serial number S/N 361765. Each cylinder has a bore of 5-1/2 inches, a stroke of 4-1/8 inches and a compression ratio of 15.4 to 16.4. The non-fired engine was driven by a dynamometer and the supercharging effect was measured in terms of compression pressure. The valve timing is such that the exhaust valve opens at 50° BBC and closes at 22° ATC and the inlet valve opens at 35° BTC and closes at 37° ABC with normal operating clearances of .0215 inches at the valves. The normal cold engine valve clearances of .016 inches for the inlet and .029 inches for the exhaust were used. Since the water jacket temperature was maintained near the normal operating range, the inlet valve timing would be expected to be very close to that of normal operating timing. The deviation from normal exhaust operating timing should have little effect since the induction process sees only the change in the overlap period.

Certain engine modifications were made for the purpose of the tests run. The thermostat was removed and the water jacket temperature was

manually held to between 155°F and 163°F. The fuel pump, injector plungers and the push rods and rocker arms for the injectors were removed. The injector nozzles were replaced with caps having .015 inch diameter holes in the tips, and copper tubing was sealed in the injector bodies and run through the valve covers. The inlet manifold was removed and replaced with adaptors made for the various pipe and tubing used. The pipe extended into the port as far as possible in all cases. A Kistler Model 601 pressure pick-up was mounted in cylinder number 3; an adaptor had already been installed in the engine.

The engine was coupled to and driven by a General Electric DC dynamometer. A Bendix Aviation Corporation Autosyn Motor Type 1, driving a Standard Electric Time Company revolution counter and timer, was used to determine the RPM. The equipment used to determine the effective port length was a Brüel & Kjær Beat Frequency Oscillator Type 1022, a Brüel & Kjær eight-inch speaker and a Tektronix Type 502A Beam Oscilloscope.

CHAPTER III

LINEARITY AND REPEATABILITY OF PRESSURE MEASURED

The pressure reading taken was the pressure built up in a pot which was separated from the cylinder by a .015 inch hole. This pressure can be seen to be linearly related to the pressure in the cylinder when the inlet valve closes if the compression and expansion processes are polytropic and the flow out of the pot into the cylinder is choked while either valve is open. The compression and expansion processes in an internal combustion engine have been shown to be polytropic processes for all practical purposes. With the pot pressure obtained and the engine valve timing used, the flow out of the pot was definitely choked during the valve events.

Looking at the non-dimensionalized curve of the cylinder pressure in Figure 2 on page 14 will aid the explanation of this relationship. Since the compression and expansion processes are polytropic the portion of the P_c/P_1 curve between the closing of the inlet valve and the opening of the exhaust valve will remain unchanged when P_1 changes.

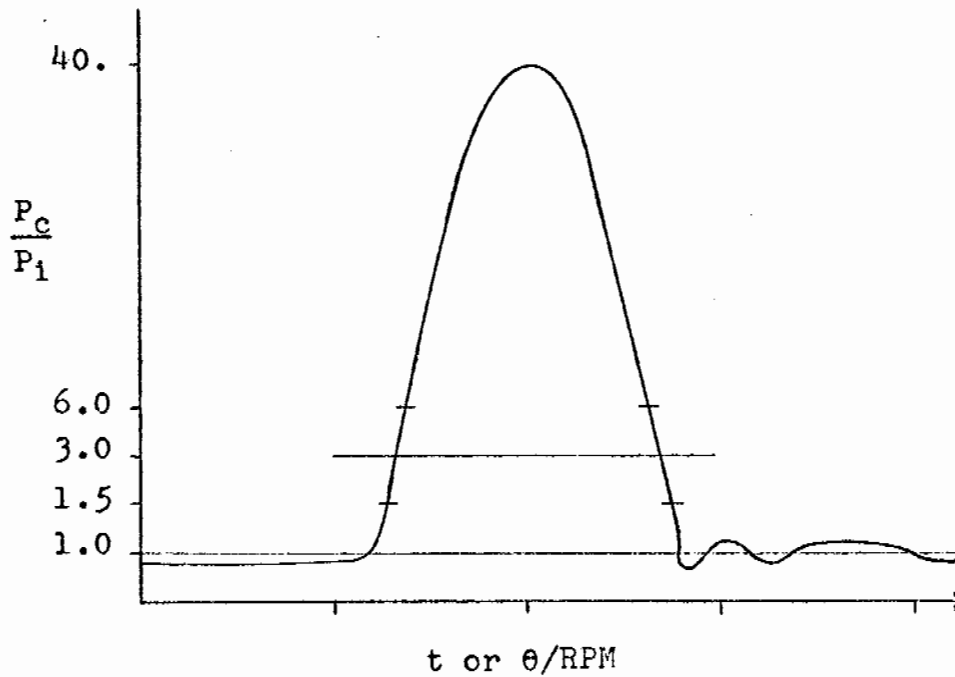


Figure 2

where P_c cylinder pressure
 P_p pot pressure
 P_1 cylinder pressure
when inlet valve closes
 t time
 θ crank angle
RPM assumed constant

Now if P_p/P_1 were to decrease with a change in P_1 then there would be more time for a relatively higher flow into the pot (as compared to flow out of the pot) and less time for flow out of the pot, which is entirely inconsistent with a decrease in P_p/P_1 . Likewise, if P_p/P_1 were to increase with a change in P_1 there would be less time for a

relatively lower flow into the pot and more time for flow out of the pot, which is inconsistent with an increase in P_p / P_1 .

A more rigorous analytical analysis using:

$$\frac{w}{A} = \sqrt{\frac{k}{R} \left(\frac{2}{k+1} \right)^{\frac{k+1}{k-1}} \frac{P_o}{\sqrt{T_o}}}$$

for choked flow, and:

$$\frac{w}{A} = \sqrt{\frac{2k}{R(k-1)}} \frac{P_o}{\sqrt{T_o}} \left(\frac{P}{P_o} \right)^{\frac{1}{k}} \sqrt{1 - \left(\frac{P}{P_o} \right)^{\frac{k-1}{k}}}$$

for non-choked flow⁽²³⁾ shows that, although the pot pressure is linearly related to the initial cylinder pressure, the square root of the ratio of the pot temperature to initial cylinder temperature effects the constant of proportionality. The resulting variation in the constant of proportionality can be seen to be very small, when the facts that the pot temperature tends to rise and fall with the inlet temperature and the total variation in inlet temperature was only four percent, are considered. Thus the variation in the constant of proportionality between the pot pressure

and the initial cylinder pressure from its mean value would be expected to be on the order of one percent or less.

The linearity between the pot pressure and the initial cylinder pressure was checked experimentally. The peak cylinder pressure was measured with the Kistler pressure pick-up. The plot of the oscilloscope output versus pot pressure in Figure 3 shows that the peak cylinder pressure and pot pressure are linearly related to within the readability of the oscilloscope.

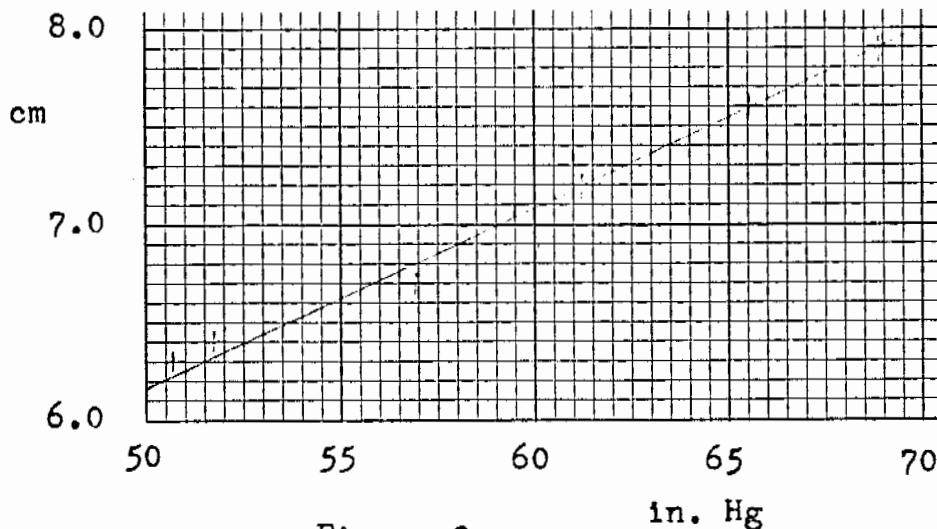


Figure 3

As stated before the compression process has been shown to be polytropic so that the peak cylinder pressure and initial cylinder pressure are linearly related. Thus the pot pressure measured should be linearly related to the initial cylinder pressure.

The error introduced by the readability of the instruments used is negligible. The experimental error, therefore, will be considered associated only with repeatability. In order to check repeatability, cylinder number three had a constant inlet configuration throughout the test except when the stock manifold was run. This configuration consisted of 4-1/8 inches of 1-1/2 inch pipe extended into the port as far as possible and fitted with a nozzle one inch long. The variations in the pressure ratios from cylinder number three were always less than ± 1 percent and less than $\pm 1/2$ percent about 75 percent of the time for any given day. Thus under similar conditions the tests are seen to be very repeatable.

The variations in pressure ratios of cylinder number three from day to day were always less than ± 3 percent and less than $\pm 1-1/2$ percent about 75 percent of the time. The day to day variations are felt to be a result of four things:

1. The tests were run over a period of four months, thus the climate changed considerably.
2. The engine thermostat was removed part way through the tests to facilitate water jacket temperature control.

3. The exhaust system had to be modified part way through the tests.
4. The head on the test side of the engine had to be pulled before the tests were completed.

NEEDED ADDITIONAL CALCULATIONS AND RESULTS

The length which should be used to compute the natural frequency of a Helmholtz resonator (page 7) is not the true pipe length because a quantity of air at the mouth of the pipe acts as a part of the system. Wood states that this correction should be $\frac{\pi}{2} R$. He also specifies similar length corrections for organ pipes of .8 R for infinite flanged ends and .6 R for normal tubes. When making end corrections for non-circular tubes the hydraulic radius was used. The end corrections for the pipes used are tabulated in Table 1 on page 41 . It should be noted that when a nozzle is used the nozzle length should be subtracted from the correction length.

The effective length of the port must also be taken into account. In order to estimate the effective port length the natural frequencies of several inlet tubes were found with the inlet valve closed. The results of this test, along with the calculation of the effective port volumes, are in Table 2 on page 42. The 1-1/2 inch pipe and the 1-1/2 x 2-1/2 inch tube extend into the port different amounts though. In this region the port cross-sectional area is about 4 square inches.

Table 3 on page 43 gives the distances the various tubes used extended into the ports, the resulting port volumes and the effective port lengths for the different inlet tubes used.

The total length corrections will thus be the sum of the end correction and the port correction. The values of total length correction for the various tubes used are given in Table 4 on page 44.

The effective A/L for pipes of non-constant area should be obtained through the formula

$$\frac{L}{A} \Big|_{\text{effective}} = \sum \frac{L_i}{A_i}$$

where i refers to a section of constant area. For computational purposes half of the length of the tapered connection, with a 30° included angle, between the different diameter pipes was considered a length of the larger pipe and half of it was considered a length of the smaller pipe. The entrance length correction was taken to correspond to the size of pipe nearest the nozzle. The effective port length was found to give best data correlation when it was taken to correspond to the smallest diameter pipe used in the inlet tube. Table 5 on page 45 gives the results of the calculation of the effective L/A for the pipes of non-constant area.

The graphs of the data from the 1-5/8 x 1-5/8 inch tube and the 1-1/2 x 2-1/2 inch tube have significant ripples and even multiple peaks. These ripples can be seen to be associated with the organ pipe type of resonance by plotting the RPM's at which the maximums and minimums of this area occur versus the particular tube length. The RPM's plotted have been corrected to a reference temperature of 85°F. Since the speed of sound in feet per second equals $49\sqrt{T}$, the corrected RPM would be:

$$\sqrt{\frac{545}{460 + T_{\text{inlet}}}} \text{ RPM measured.}$$

The curves in Figure 4 on page 22 correspond to the maximums and minimums as predicted by

$$L = \frac{360 \text{ c}}{N \times \text{RPM}}$$

from page 2 with c taken as 1,143 feet per second and the values of N specified. It should be noted that the fractional values of N correspond to curves which should predict minimums. Although the equation does not predict the maximums and minimums exactly, it is obvious from Figure 4 that the data has the same functional relationship between tube length and RPM. Thus the ripples in the data are associated with an organ pipe type of resonance, and their effect can be negated by drawing a smoothed

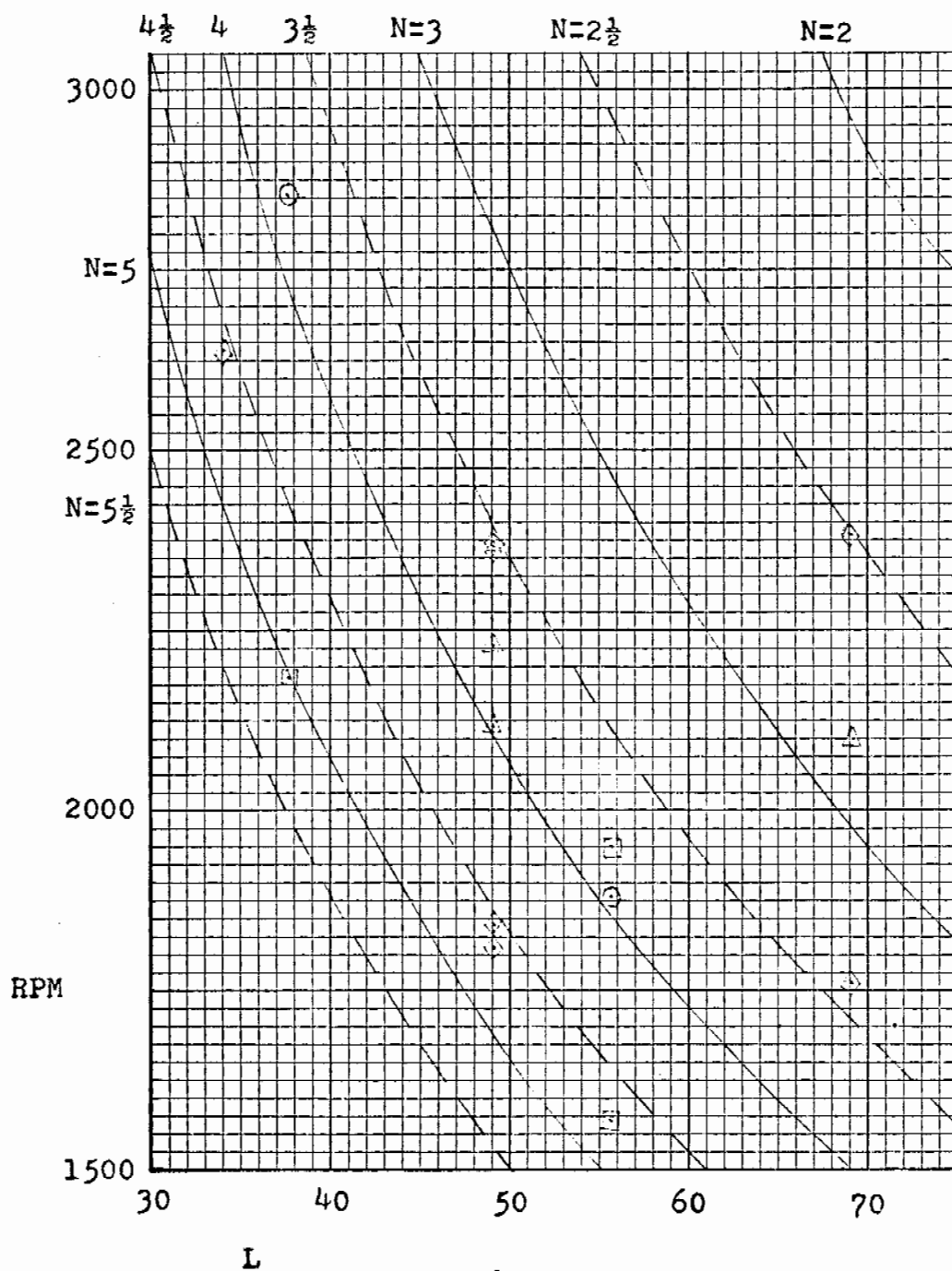


Figure 4

- ◇ $1\frac{1}{2} \times 2\frac{1}{2}$ tube, max.
- △ $1\frac{1}{2} \times 2\frac{1}{2}$ tube, min.
- $1\frac{5}{8} \times 1\frac{5}{8}$ tube, max.
- $1\frac{5}{8} \times 1\frac{5}{8}$ tube, min.

curve through the data. It should be noted that the organ pipe type of resonance did not become noticeable until the volume of the inlet system was $3/4$ of the cylinder volume or larger.

CHAPTER IV

OTHER DATA

An inspection of the literature produces some data which can be correlated to the Helmholtz approach. The correlation will be analyzed by seeing whether or not k is a constant for a given engine and what its range is for various engines. Solving for k in the equation on page 9:

$$k = \frac{162 \times c}{\text{RPM}} \sqrt{\frac{A}{L_e V}} \sqrt{\frac{R-1}{R+1}}$$

Matthews and Gardiner⁽¹⁾ obtained data from a five-inch bore, seven-inch stroke engine with a compression ratio of 11.4. The inlet pipe used had a diameter of 2-1/8 inches and a port volume of roughly 20 cubic inches. Thus the total length correction would be $5.6 + 1.7 = 7.3$ inches. Assuming that c is 1,140 feet per second and solving for k :

$$k = \frac{27,200}{\text{RPM} \sqrt{L_e}}$$

L	L_e	RPM	k
70	77.3	1340	2.31
60	67.3	1465	2.26
50	57.3	1585	2.26
40	47.3	1800	2.20

This data correlates well with the theory and gives an average k of 2.26.

Dennison⁽⁵⁾ used two engines to obtain his data; both had a 12-inch stroke; one had an 8-1/4 inch bore and the other had a 9-inch bore. Since one had a compression ratio of 11.8 and the other 13.0 (correspondence is unknown) a compression ratio of 12.4 will be used and will introduce an error of less than one half of one percent. Assuming c is 1,140 feet per second and taking the entrance effects into account:

$$k = \frac{49,200}{\text{RPM} \times \sqrt{L + \frac{\pi D}{4}}} \times \frac{D}{B}$$

D-Diameter	B-Bore	L	RPM	k
2.00	8.25	36	800	2.43
2.50	8.25	66	800	2.26
3.00	9.00	52	1000	2.22

It can be seen that k is larger than expected and non-linear, and that taking an effective port length into account would reduce both the magnitudes of the k 's and their scatter. An assumption of 40 cubic inches for the port volume is not unreasonable in

view of the size of this engine compared to that used by Matthews and Gardiner⁽¹⁾. This assumption gives the following results:

L	L _{port}	L _e	k
36	12.7	50.3	2.10
66	8.1	76.1	2.14
52	5.6	60.0	2.12

with an average of k equal to 2.12.

Morse, Boden and Schechter⁽⁶⁾ obtained data from a 137.6 cubic inch engine with a compression ratio of five. An inlet pipe of 2.56 inch diameter was used; the engine was operated at 1,220 RPM and the velocity of sound in the inlet air was 1,100 feet per second. The size of this engine is within a few tenths of a cubic inch of that of the engine used by Matthews and Gardiner, thus an assumption of twenty cubic inches for the port volume would seem reasonable. The total length correction would be $3.9 + 2.0 = 5.9$. The resulting optimum pipe length of one hundred inches gives a k of 2.60. This value of k is high but the valve timing of the test engine was unusual; the inlet opened at top dead center and closed at bottom dead center. This valve timing significantly decreases the period of the induction

process and thus would be expected to increase the value of k obtained relative to a more conventionally timed engine.

Engelman⁽²⁰⁾ used an engine with a 2-1/4 inch bore, a 2-1/4 inch stroke and a compression ratio of five. He also investigated the data Ricardo⁽³⁾ obtained from an engine with a displacement of 538 cubic inches. He recommended the use of 2.1 as the value of k .

Downing⁽¹⁵⁾ obtained data from a racing engine with a displacement of 35.0 cubic inches per cylinder and one inlet per cylinder. Assuming that the inlet temperature was 85°F and the compression ratio was 10.5 should introduce no more than 2 percent error for reasonable variations in these parameters.

$$k = \frac{25,300}{\text{RPM}} \sqrt{\frac{D}{L_e}}$$

For the pipe with a 1.575 inch diameter:

L	L_e	RPM	k
5.25	6.5	5000	3.13
8	9.2	4350	3.02
11	12.2	4150	2.75
21.5	22.7	3650	2.29
35.5	36.7	2100	2.27

For the pipe with a 1.970 inch diameter:

L	L_e	RPM	k
5.25	6.8	4850	3.94
11	12.5	4725	2.98
15	16.5	4450	2.76
21.5	23.0	4000	2.60
32.5	34.0	3500	2.44

An assumed effective port length of 8 inches for the 1.575 inch pipe and 12 inches for the 1.97 inch pipe yields:

1.575 inch diameter			1.970 inch diameter		
L	L_e	k	L	L_e	k
5.25	14.5	2.09	5.25	18.8	2.37
8	17.2	2.21	11	24.5	2.13
11	20.2	2.16	15	28.5	2.10
21.5	30.7	1.97	21.5	35.0	2.11
35.5	44.7	2.06	32.5	46.0	2.10

Looking at the sketch of the system that Downing gives, the assumed effective lengths of the port and pipe adaptors are not unreasonable. This data thus gives an average k of 2.13.

The analysis on the data found in the literature substantiates the Helmholtz resonator

approach and suggests that for conventional engines k would be around 2.1 or 2.2.

TEST RESULTS

Figures 8 through 24 in the appendix are plots of the pressure ratios obtained for the various inlet configurations. Figure 5 page 32 is a plot of the RPM at which the peak pressure ratio occurred versus the square root of the effective A/L for the specific inlet used. Here again, the RPM's have been corrected to a reference temperature of 85°F by using:

$$\sqrt{\frac{545}{460 + T_{\text{inlet}}}} \text{ RPM}_{\text{measured}}.$$

This data can be represented by a straight line which goes through the origin as the Helmholtz resonator approach predicts. The best straight line, according to a least squares fit, is:

$$N = 7877 \sqrt{\frac{A}{L}} + 36$$

Neglecting the constant term, the value of k which this data yields is 2.23.

The percent supercharge at the corrected RPM at which the pressure ratio peaked was computed by dividing the pressure ratio of the test inlet by the pressure ratio of the stock manifold at that RPM. Figure 6 page 33 shows two trends. The first is that, for any given type of inlet, as the RPM at which the system peaks increases the amount of maximum super-

charge decreases. The second is that as the area of the inlet decreases the amount of maximum supercharge decreases.

The amount of supercharge obtained is indeed impressive when the cost in terms of increased pumping work is considered. Figure 7 page 34 is a plot of the corrected RPM at which the pressure ratio was maximum versus the power required at this RPM for the various inlets used. The curve is the power required with the stock inlet manifold.

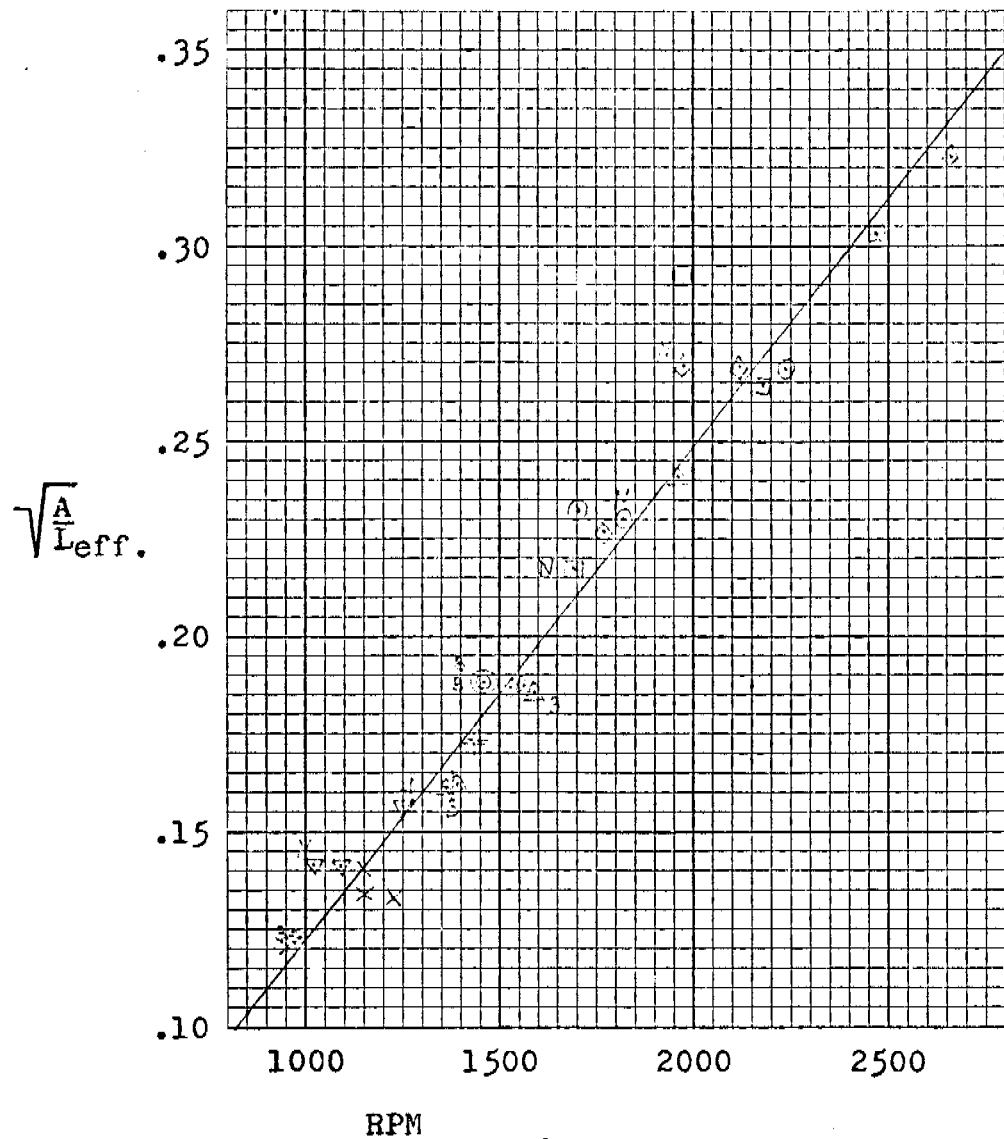


Figure 5

- ◇ 1-1/2 x 2-1/2 tube
- ▣ 1-5/8 x 1-5/8 tube
- ⊙ 1 1/2 pipe
- △ 1 1/4 pipe
- ▽ 1 pipe
- + sectioned pipe, 1 1/4 min.
- × sectioned pipe, 1 min.
- N, no nozzle
- B, pipe with bend

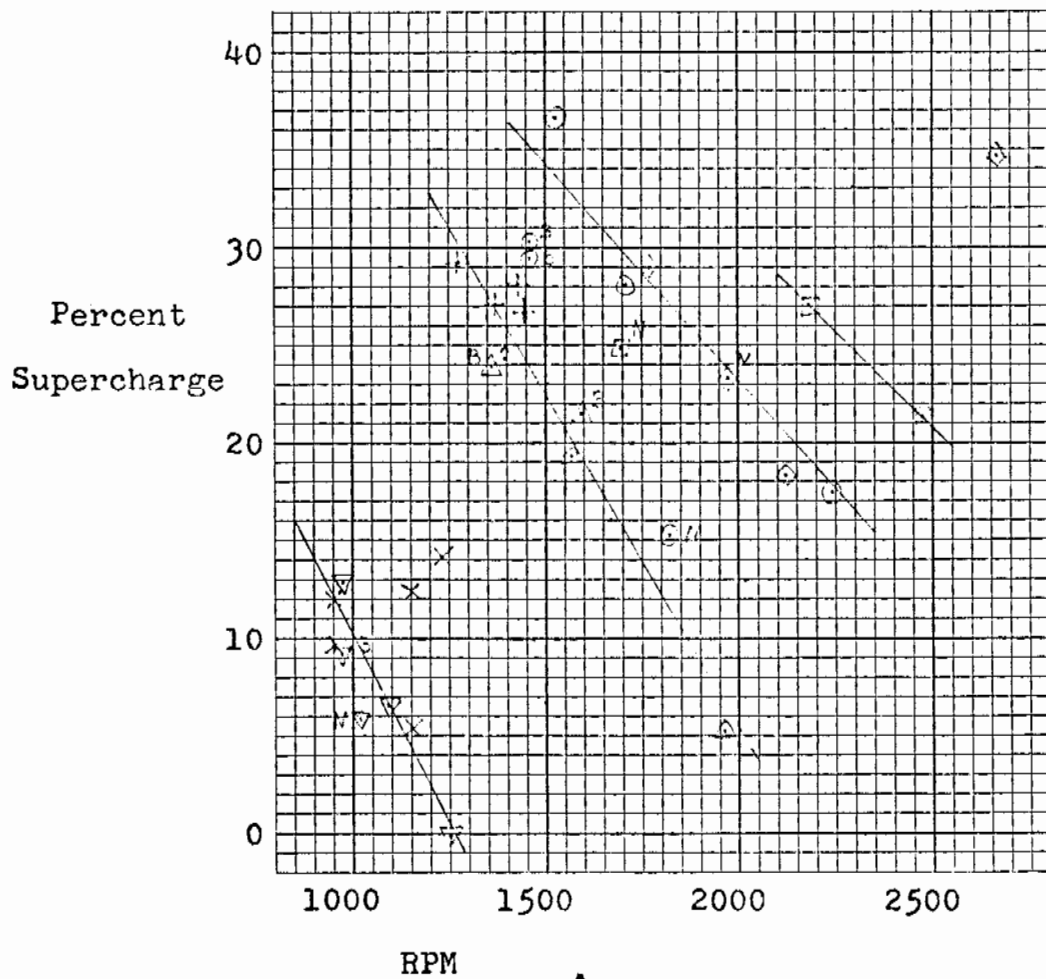


Figure 6

- ◇ 1-1/2 x 2-1/2 tube
- 1-5/8 x 1-5/8 tube
- ⊙ 1 1/2 pipe
- △ 1 1/4 pipe
- ▽ 1 pipe
- + sectioned pipe, 1 1/4 min.
- × sectioned pipe, 1 min.
- N, no nozzle
- B, pipe with bend

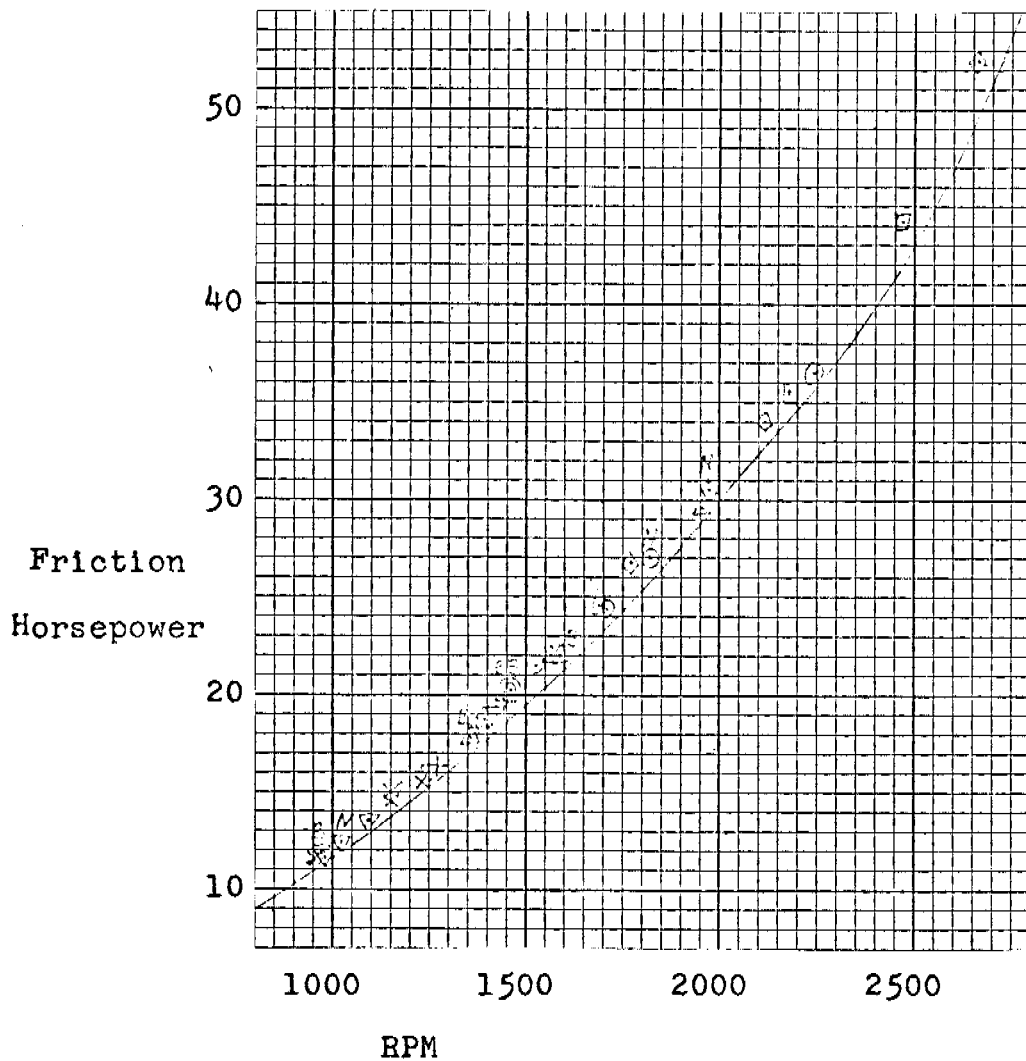


Figure 7

- 1-1/2 x 2-1/2 tube
- 1-5/8 x 1-5/8 tube
- 1 1/2 pipe
- 1 1/4 pipe
- 1 pipe
- sectioned pipe, 1 1/2 min.
- sectioned pipe, 1 min.
- N, no nozzle
- B, pipe with bend

CHAPTER V

CONCLUSIONS

Although the effects of the organ pipe type of resonance become significant when the volume of the inlet system becomes eighty percent of the cylinder volume or more, this type of resonance is not the dominant phenomenon. The most significant changes in the breathing of an engine are the result of the resonance of the induction system as a Helmholtz resonator. The speed at which the maximum gain in breathing occurs can be predicted from the equation:

$$\text{RPM} = \frac{162}{k} c \sqrt{\frac{A}{L_e V}} \sqrt{\frac{R-1}{R+1}}$$

where

k	2.1 or 2.2 for most conventional engines
c	speed of sound in air, feet per second
A	area of inlet tube, square inches
V	displacement volume of engine, cubic inches
L_e	effective length of the inlet tube, inches, see pages 19 and 20 for computation of the total effective length of the inlet system
R	compression ratio

This equation is good for inlet tubes of various areas, lengths, shapes; for tubes with abrupt or well-rounded entrances; for inlet tubes of non-constant cross-sectional area; and for curved inlet tubes where the ratio of the radius of curvature of the bend to the radius of the tube is larger than ten.

BIBLIOGRAPHY

1. Matthews, R., Gardiner, A. W., "Increasing the Compression Pressure In An Engine By Using A Long Intake Pipe", N.A.C.A. Technical Note 180, 1924.
2. Capetti, A., "Effect Of Intake Pipe On The Volumetric Efficiency Of An Internal Combustion Engine", N.A.C.A. Technical Memorandum 501, 1927.
3. Ricardo, H. R., U. S. Patent #1,834,473 December 1, 1931.
4. List, H., "Increasing The Volumetric Efficiency Of Diesel Engines By Intake Pipes", N.A.C.A. Technical Memorandum 200, 1932.
5. Dennison, E. S., "Inertia Supercharging Of Engine Cylinders", A.S.M.E. Transactions, CGP-55-5, pp. 53 - 64, 1933.
6. Morse, P. M., Boden, R. H., Schechter, H., "Acoustics Vibrations And Internal Combustion Engine Performance", Journal Of Applied Physics, Vol. 9, pp. 16 - 23, 1938.
7. Lutz, C., "Resonance Vibrations In Intake And Exhaust Pipes Of In-Line Engines", N.A.C.A. Technical Memorandum 952, 1940.
8. Boden, R. H., Schechter, H., "Dynamics Of The Inlet System Of A Four-Stroke Engine", N.A.C.A. Technical Note 935, 1944.
9. Kastner, L. J., "Induction Ramming Effects In Single-Cylinder Four-Stroke Engines", The Instruction Of Mechanical Engineers Proceedings, Vol. 153, pp. 206-220, 1945.
10. Binder, R. C., Hall, A. S., "An Introduction To An Analysis Of Gas Vibrations In Engine Manifolds", A.S.M.E. Transactions, Vol. 69, pp. A-183 to A-187, 1947.
11. Lichty, L. C., Internal Combustion Engines, pp. 283 - 285 and 287 - 289, McGraw - Hill Book Company, Inc., New York, 1951.

12. Platner, J. B., Moore, C. D., U. S. Patent #2,766,743, October 16, 1956.
13. Taylor, C. F., Livengood, J. C., Tsai, D. H., "Dynamics In The Inlet System Of A Four-Stroke Single-Cylinder Engine", A.S.M.E. Transactions, Vol. 77, pp. 1133 - 1145, 1955.
14. Platner, J. B., Moore, C. D., U. S. Patent #2,791,205, May 7, 1957.
15. Downing, E. W., "Petrol Injection: Some Further Developments", The Institution Of Mechanical Engineers Proceedings Of The Automobile Division, Number 6, pp. 170 - 171, 1957-58.
16. McMunn, J. C., Yoerger, E. R., Weber, J. A., "Pulsating Pressures In An Internal-Combustion Engine Induction System", Agricultural Engineering, Vol. 42, No. 9, pp. 490 - 493, 1961.
17. Clarke, J. S., "Initiation And Some Controlling Parameters Of Combustion In The Automobile Engine", S.A.E. Transactions, Vol. 70, pp. 240-261, 1962.
18. Geschelin, J., "Chrysler's Developments In Ram-Charging Of Engines", Automotive Industries, Vol. 130, No. 3, pp. 35 - 37, 1964.
19. Lichty, L. C., Combustion Engine Processes, pp. 343 - 345, 363 - 364, McGraw - Hill Book Company, New York, 1967.
20. Engelman, H. W., "Surge Phenomena In Engine Scavenging", Ph.D. Thesis, University Of Wisconsin, 1953.
21. Wood, A., Acoustics, pp. 103 - 107, 253, 406, Blackie & Son Limited, London & Glasgow, 1960.
22. Cambi, E., "Trigonometric Components Of A Frequency Modulated Wave", Proceedings I.R.E., Vol. 36, pp. 42 - 49, 1948.

23. Shapiro, A., The Dynamics and Thermodynamics of Compressible Fluid Flow, Vol. I, pp. 85, 109, The Ronald Press Company, New York, 1953.
24. Doebelin, E., Measurement Systems: Application and Design, pp. 391 - 402, McGraw - Hill, Inc., New York, 1966.

APPENDIX

Table 1

Hydraulic diameter of rectangular tube:

$$D_h = \frac{2 \times 1-13/32 \times 2-17/32}{1-13/32 + 2-17/32} = 1.810 \text{ inches}$$

Hydraulic diameter of square tube: $D_h = 1.625$ inches

Helmholtz end correction, inches

type tube	with nozzle	without nozzle
1-1/2 x 2-1/2 tube	.42	1.42
1-5/8 x 1-5/8 tube	.40	1.28
1-1/2 pipe	.26	1.26
1-1/4 pipe	.08	1.08
1 pipe	-.18 → 0	.82

Organ pipe end correction, inches

type tube	with nozzle	without nozzle
1-1/2 x 2-1/2 tube	-.35 → 0	.65
1-1/4 pipe	-.52 → 0	

Table 2

Frequency of an organ pipe closed at one end $f = \frac{c}{4L}$

@74°F solving for L in inches and f in cps $L = \frac{3400}{f}$

cylinder number two, using different lengths of
1-1/2 x 2-1/2 inch tube with nozzles:

<u>L pipe and nozzle</u>	<u>f</u>	<u>L computed</u>	<u>Effective port length</u>
25.9	100	34.0	8.1
40.9	69	49.3	8.4
61.0	50	68.0	7.0

average effective port volume $7.8 \times 3.56 = 27.8$.

cylinder number one, using different lengths of
1-1/4 inch pipe with nozzles:

<u>L pipe and nozzle</u>	<u>f</u>	<u>L computed</u>	<u>Effective port length</u>
26.9	79	43.0	16.1
41.0	61	55.7	14.7

average effective port volume $15.4 \times 1.48 = 22.8$.

Table 3

<u>type tube</u>	<u>extension into port</u>	<u>port volume</u>	<u>tube area</u>	<u>effective port length</u>
1-1/2 x 2-1/2 tube, inches	1.50		3.56	
cylinder #1		26.3		7.4
cylinder #2		27.8		7.8
1-5/8 x 1-5/8 tube, inches	2.19		2.64	
cylinder #1		23.6		8.9
cylinder #2		25.0		9.5
1-1/2 pipe	2.00		2.02	
cylinder #1		24.3		12.0
cylinder #2		25.8		12.8
1-1/4 pipe	2.38		1.48	
cylinder #1		22.8		15.4
cylinder #2		24.3		16.4
1 inch pipe	2.50		.855	
cylinder #1		22.3		26.1
cylinder #2		23.8		27.8

Table 4

Total length correction, inches

<u>type tube</u>	<u>without nozzle</u>	<u>with nozzle</u>
1-1/2 x 2-1/2 tube		
cylinder #2	9.2	8.2
1-5/8 x 1-5/8 tube		
cylinder #2	10.8	9.9
1-1/2 inch pipe		
cylinder #1	13.3	12.3
cylinder #2	14.1	13.1
1-1/4 inch pipe		
cylinder #1	16.5	15.5
cylinder #2	17.5	16.5
1 inch pipe		
cylinder #1	26.9	26.1
cylinder #2	28.6	27.8

Table 5

<u>lengths of pipe used</u>			<u>cylinder</u>	$\frac{L}{A}$ port	$\frac{L}{A}$ effective
engine -- air					
$1\frac{1}{2}$ in.	$1\frac{1}{2}$ in.	$1\frac{1}{2}$ in.			
9.2	20.5	18.0	#1	10.4	39.0
26.3	21.3		#1	10.4	38.8
1 inch	$1\frac{1}{8}$ in.	1 inch			
8.3	21.2	15.7	#1	30.5	69.0
8.3	21.6		#1	30.5	51.1
1 inch	$1\frac{1}{4}$ in.	1 inch			
8.0	14.6	15.5	#1	30.5	67.9
$1\frac{1}{8}$ in.	$1\frac{1}{2}$ in.	$1\frac{1}{2}$ in.			
4.4	14.4	21.2	#2	11.1	33.6
24.3	15.2		#2	11.1	33.4
$1\frac{1}{8}$ in.	1 inch	$1\frac{1}{8}$ in.			
4.7	9.1	21.6	#2	32.5	56.3
24.7	9.6		#2	32.5	55.9

Table 6
TEST CONDITIONS

Stock Manifold	T _{inlet}	P _{atm}	Date
	78.9	29.41	11/04/67

1-13/32 x 2-17/32 tube area = 3.56

L	T _{inlet}	P _{atm}	Date
61.0	79.0	28.97	11/24/67
40.9	82.6	29.58	12/19/67
39.9,n*	79.0	29.47	12/22/67
25.9	80.6	29.51	12/22/67

1-5/8 x 1-5/8 tube area = 2.64

L	T _{inlet}	P _{atm}	Date
45.0,n	77.7	29.36	11/04/67
27.9	90.7	29.19	12/21/67
18.8	81.2	29.49	12/22/67

1.604 pipe area = 2.02

L	T _{inlet}	P _{atm}	Date
45.0	81.6	29.05	10/18/67
44.1, b-27*	84.2	29.32	12/21/67
44.1, b-7	86.9	29.59	12/19/67
25.1	95.9	29.65	9/05/67
24.1,n	85.5	29.57	12/19/67
15.1	95.6	29.65	9/05/67

*n - denotes no nozzle.

*b-27 - denotes 27 inches to bend.

Table 6 (continued)

1.374 pipe			area = 1.48	
L		T _{inlet}	P _{atm}	Date
41.4, b-11		79.0	29.47	12/22/67
41.0		84.2	29.32	12/21/67
27.5, b-11		80.6	29.51	12/22/67
26.9		87.4	29.28	12/21/67
10.0		90.7	29.19	12/21/67
1.043 pipe			area = .855	
L		T _{inlet}	P _{atm}	Date
32.0, b-10		82.6	29.58	12/19/67
31.0		81.6	29.05	10/18/67
16.8		77.7	29.36	11/04/67
15.8, n		79.0	28.97	11/24/67
8.7		85.9	29.07	12/18/67
Sectioned pipes				
1 $\frac{1}{2}$	1 $\frac{1}{4}$	1 $\frac{1}{2}$	T _{inlet}	P _{atm} Date
4.4	14.4	21.2	87.4	29.28 12/21/67
24.3	15.2		88.4	29.22 12/21/67
1 $\frac{1}{4}$	1 $\frac{1}{2}$	1 $\frac{1}{4}$		
9.2	20.5	18.0	81.2	29.49 12/22/67
26.2	21.3		88.4	29.22 12/21/67

Table 6 (continued)

Sectioned pipes			T_{inlet}	P_{atm}	Date
$1\frac{1}{2}$	1	$1\frac{1}{2}$			
4.7	9.1	21.6	85.9	29.07	12/18/67
24.7	9.6		86.8	29.13	12/18/67
1	$1\frac{1}{2}$	1			
8.3	21.2	15.7	86.9	29.59	12/19/67
8.3	21.6		86/8	29.13	12/18/67
1	$1\frac{1}{4}$	1			
8.0	14.6	15.5	85.5	29.57	12/19/67

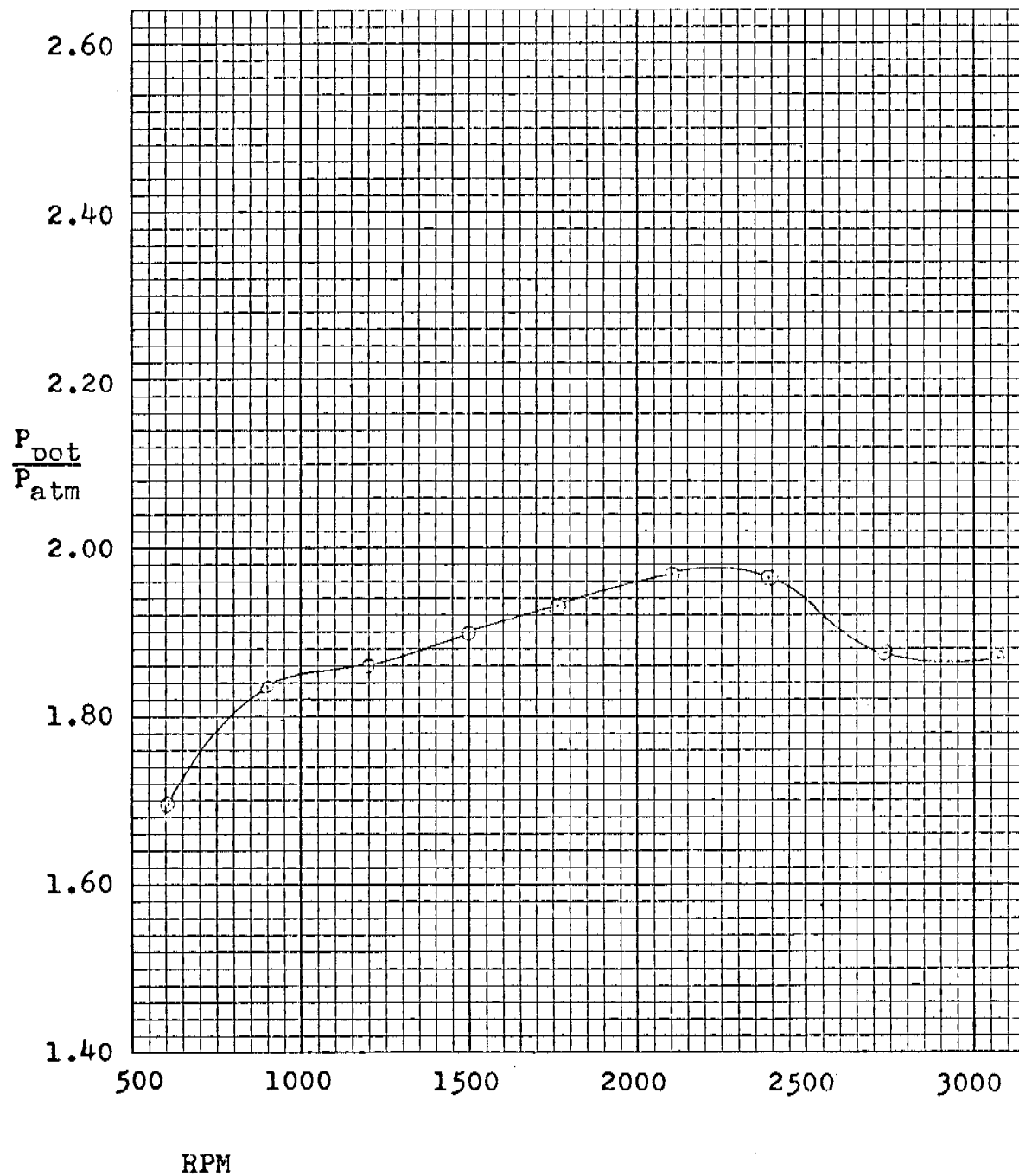


Figure 8

⊙ Stock Manifold,
average of the three
pressure readings

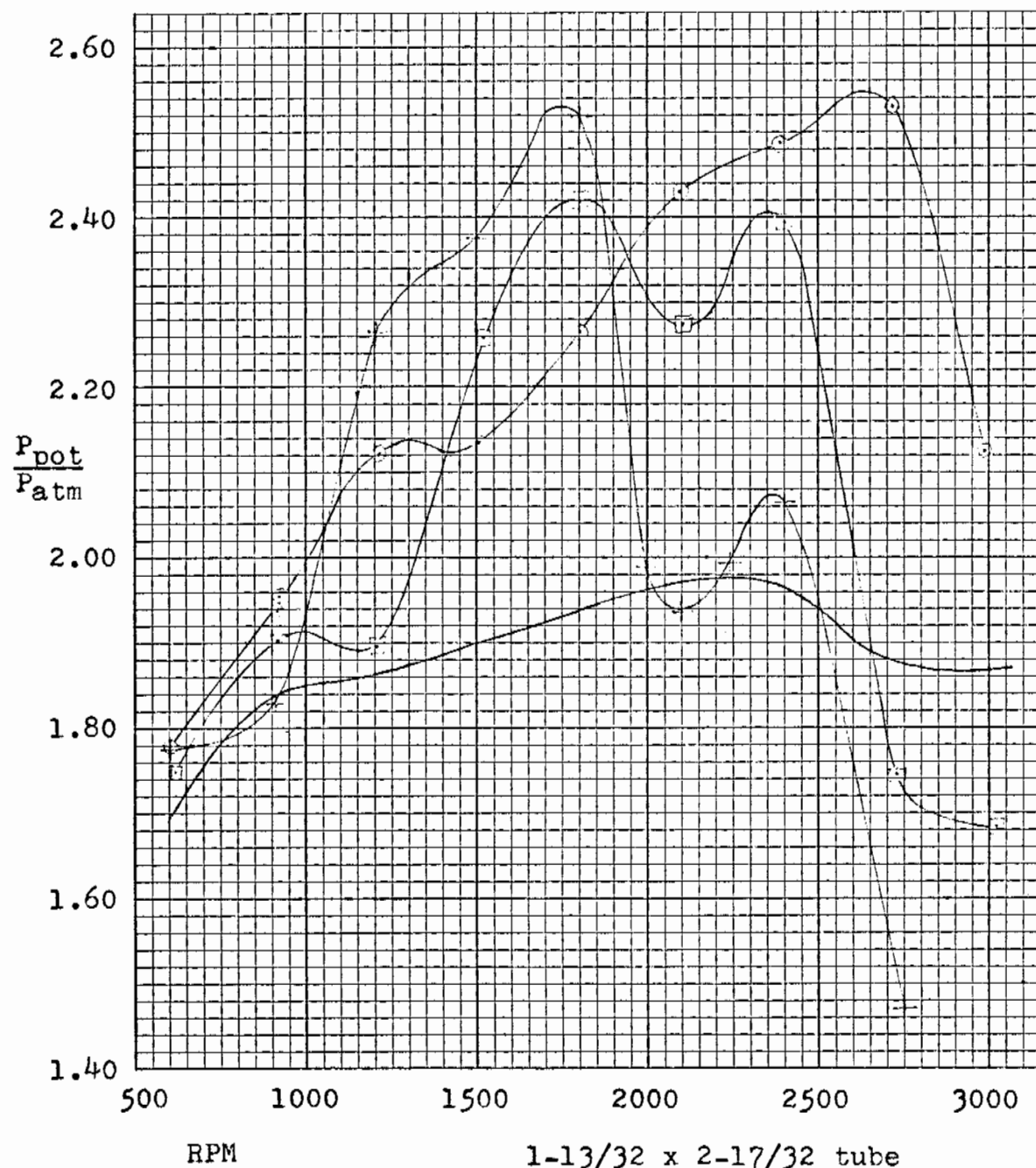


Figure 9

1-13/32 x 2-17/32 tube

cyl # length

2 + 61.0

2 □ 40.9

2 ⊙ 25.9

— Stock Manifold

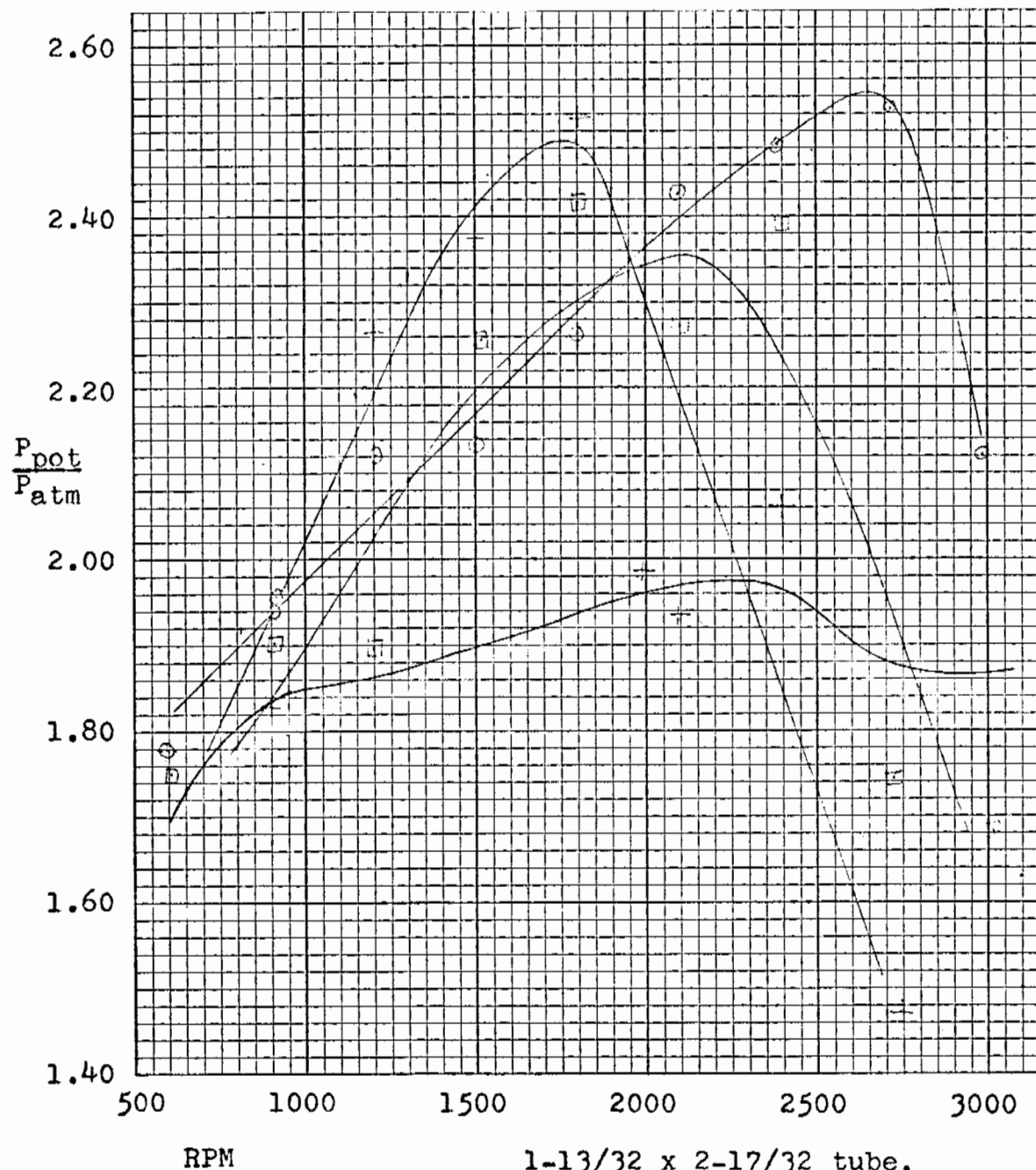


Figure 10

1-13/32 x 2-17/32 tube,
smoothed curve

cyl # length

2 + 61.0

2 □ 40.9

2 ○ 25.9

— Stock Manifold

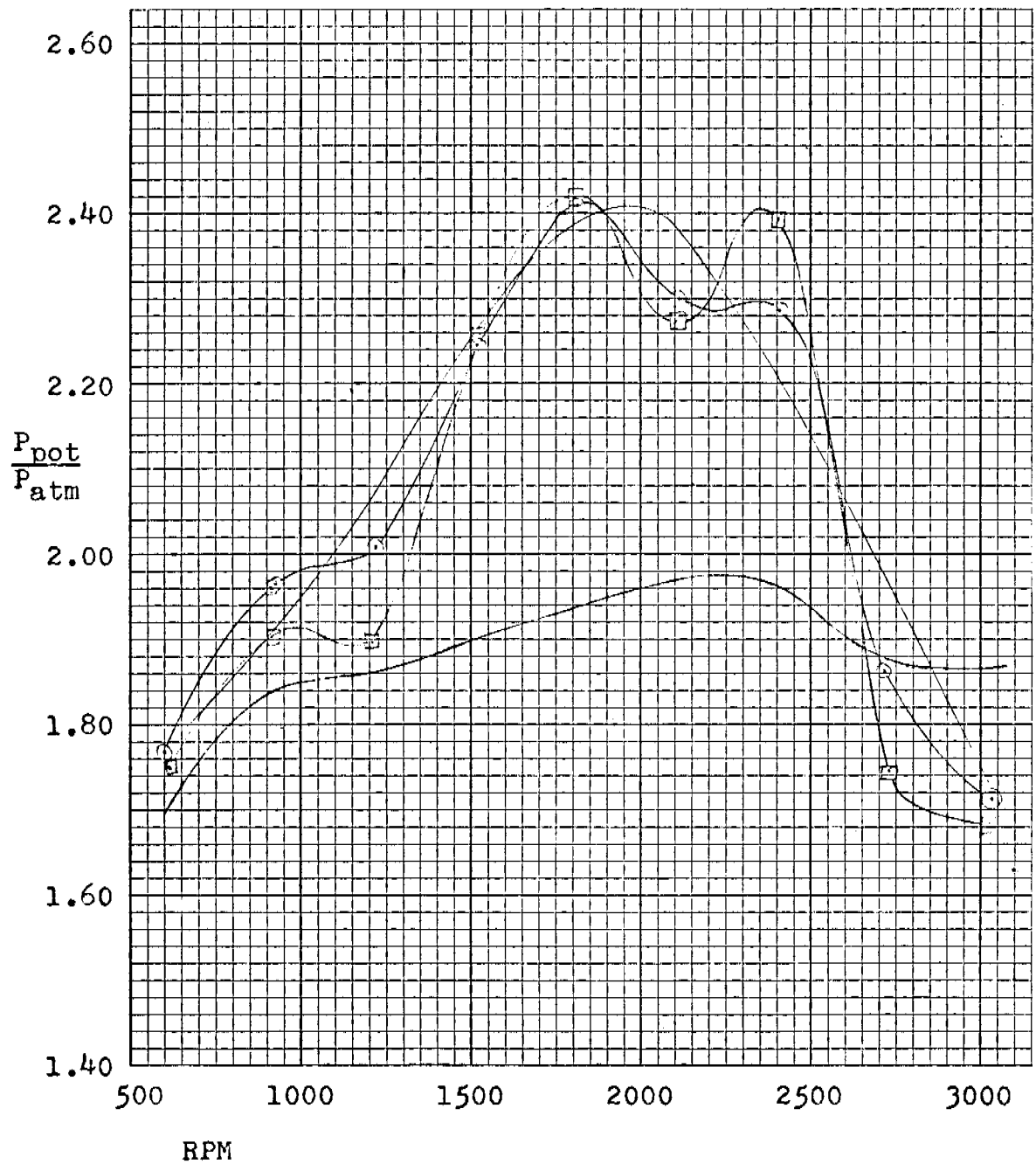


Figure 11

1-13/32 x 2-17/32 tube

cyl # length

2 □ 40.9

2 ○ 39.9, no nozzle

— Stock Manifold

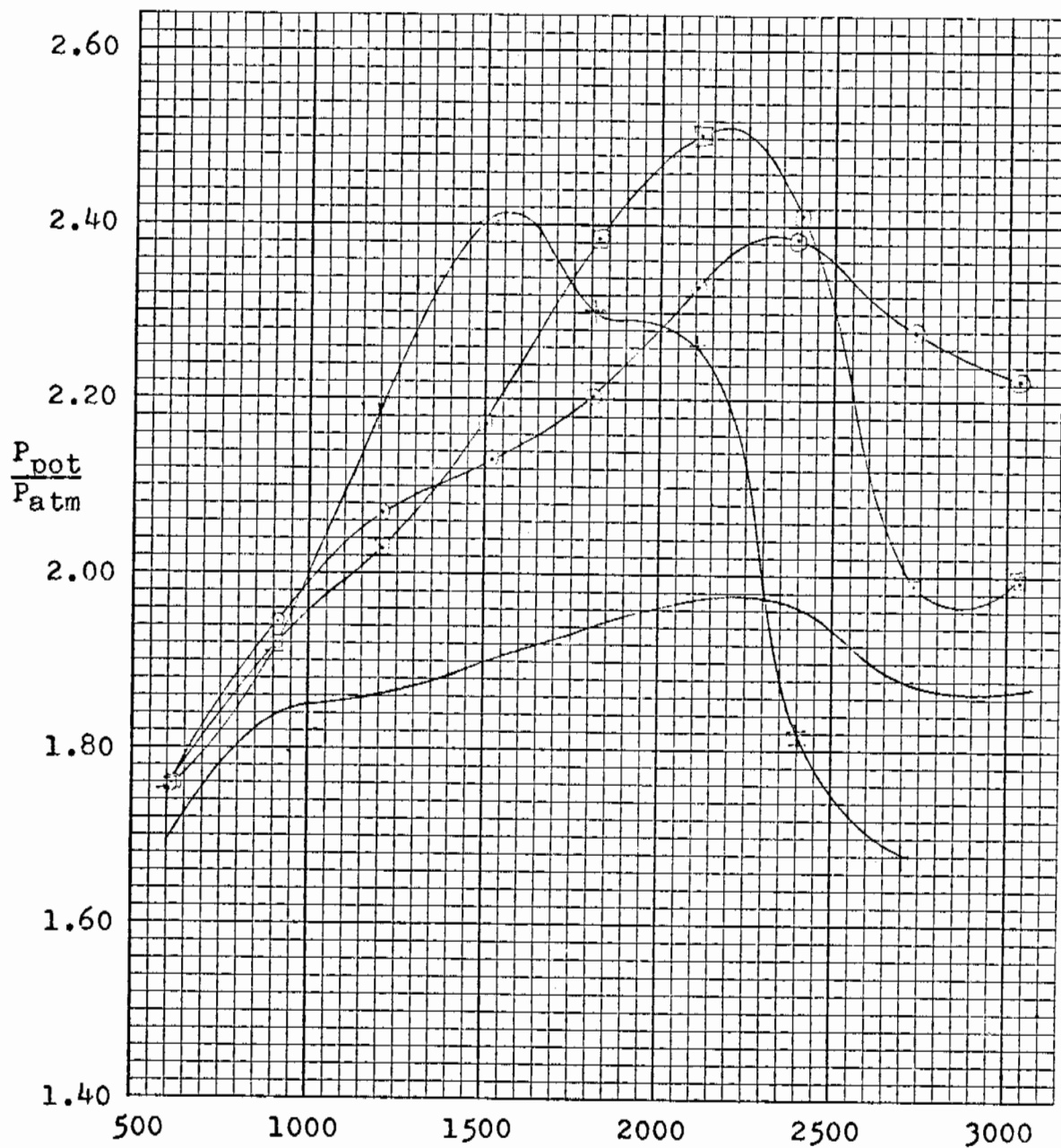


Figure 12

1-5/8 x 1-5/8 tube

cyl # length

2 + 45.0, no nozzle

2 □ 27.9

2 ○ 18.8

— Stock Manifold

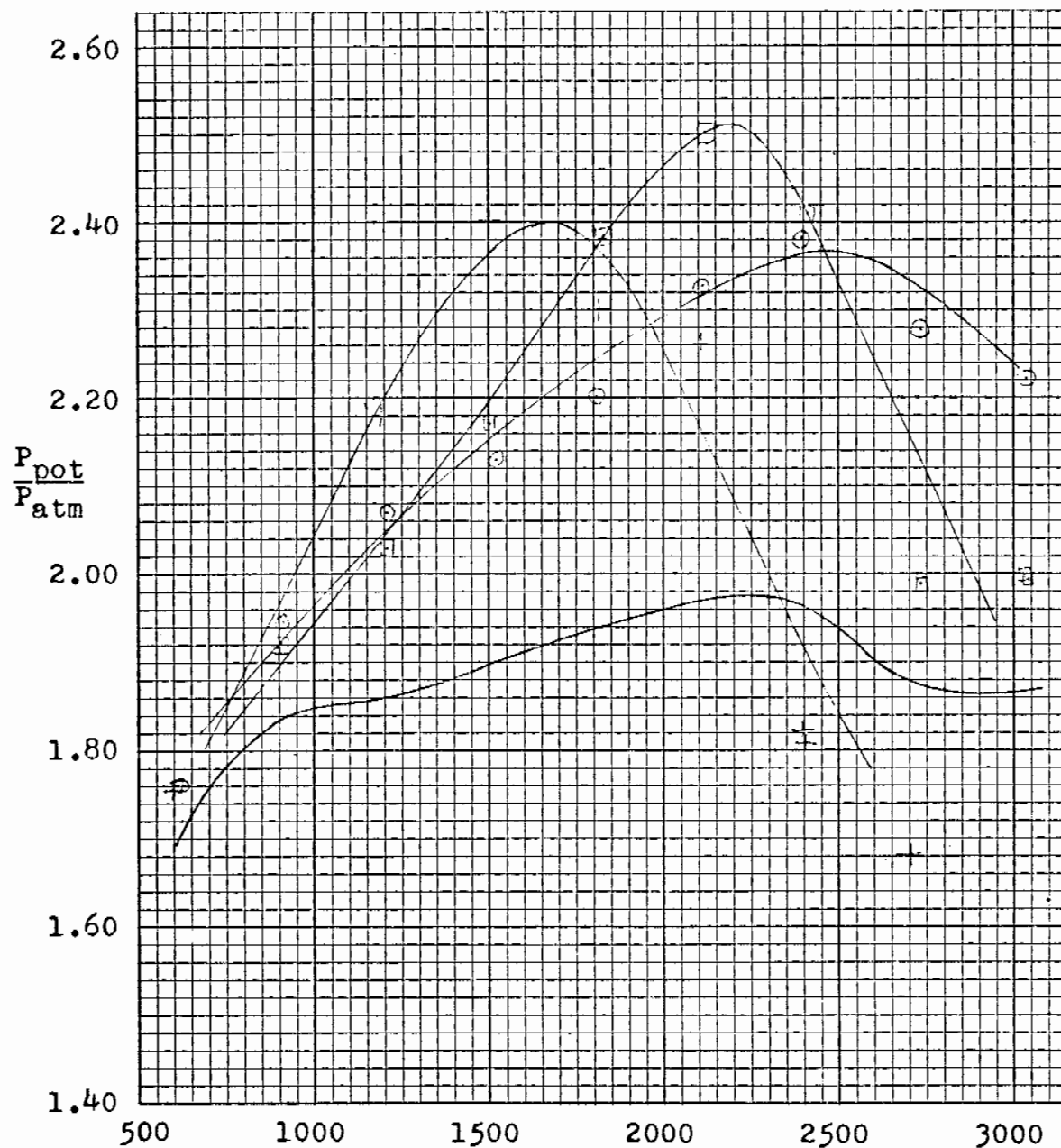


Figure 13

1-5/8 x 1-5/8 tube,
smoothed curve

cyl # length

2 + 45.0, no nozzle

2 □ 27.9

2 ○ 18.8

— Stock Manifold

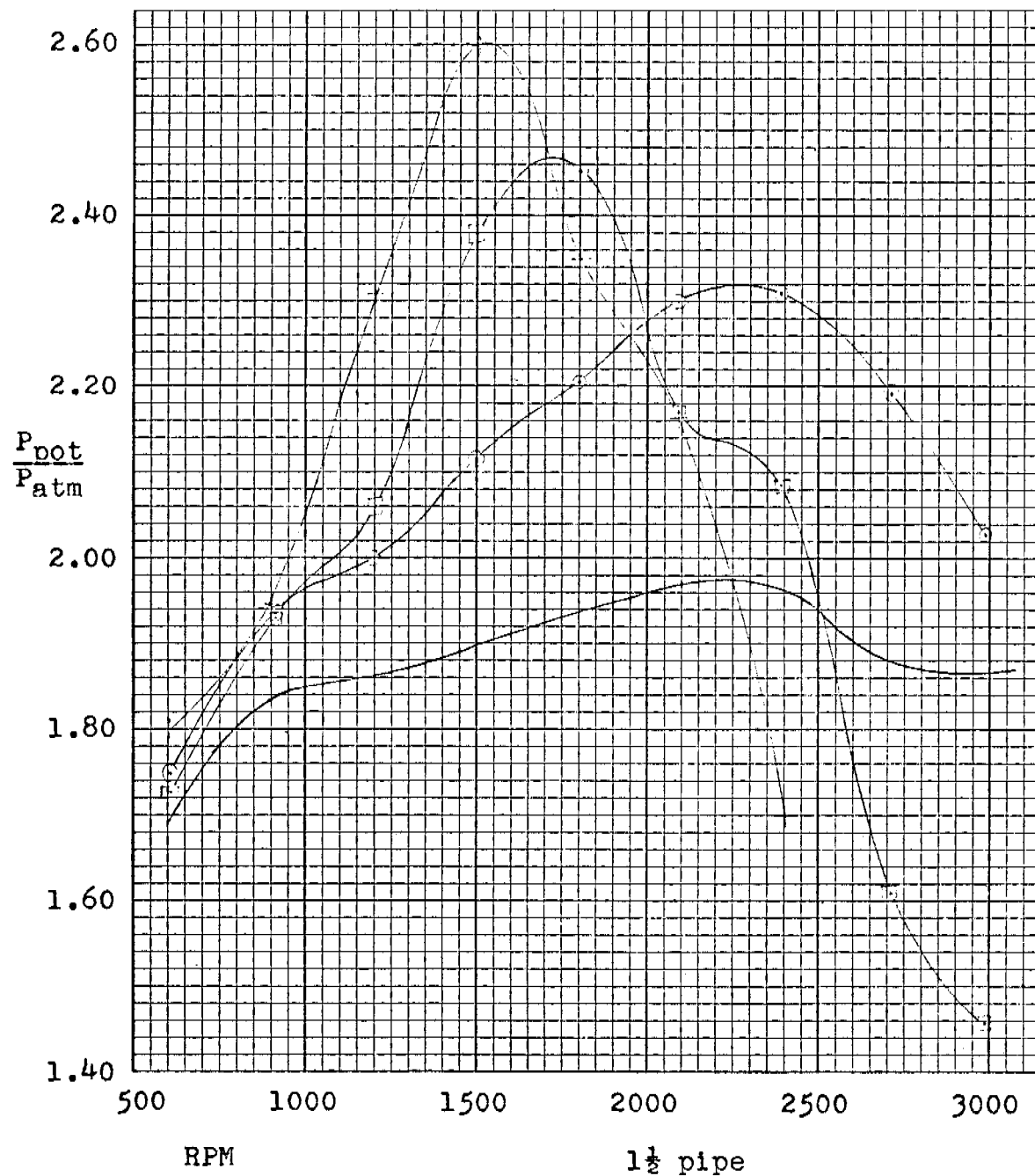


Figure 14

cyl # length

2 + 45.0

1 □ 25.1

2 ⊙ 15.1

— Stock Manifold

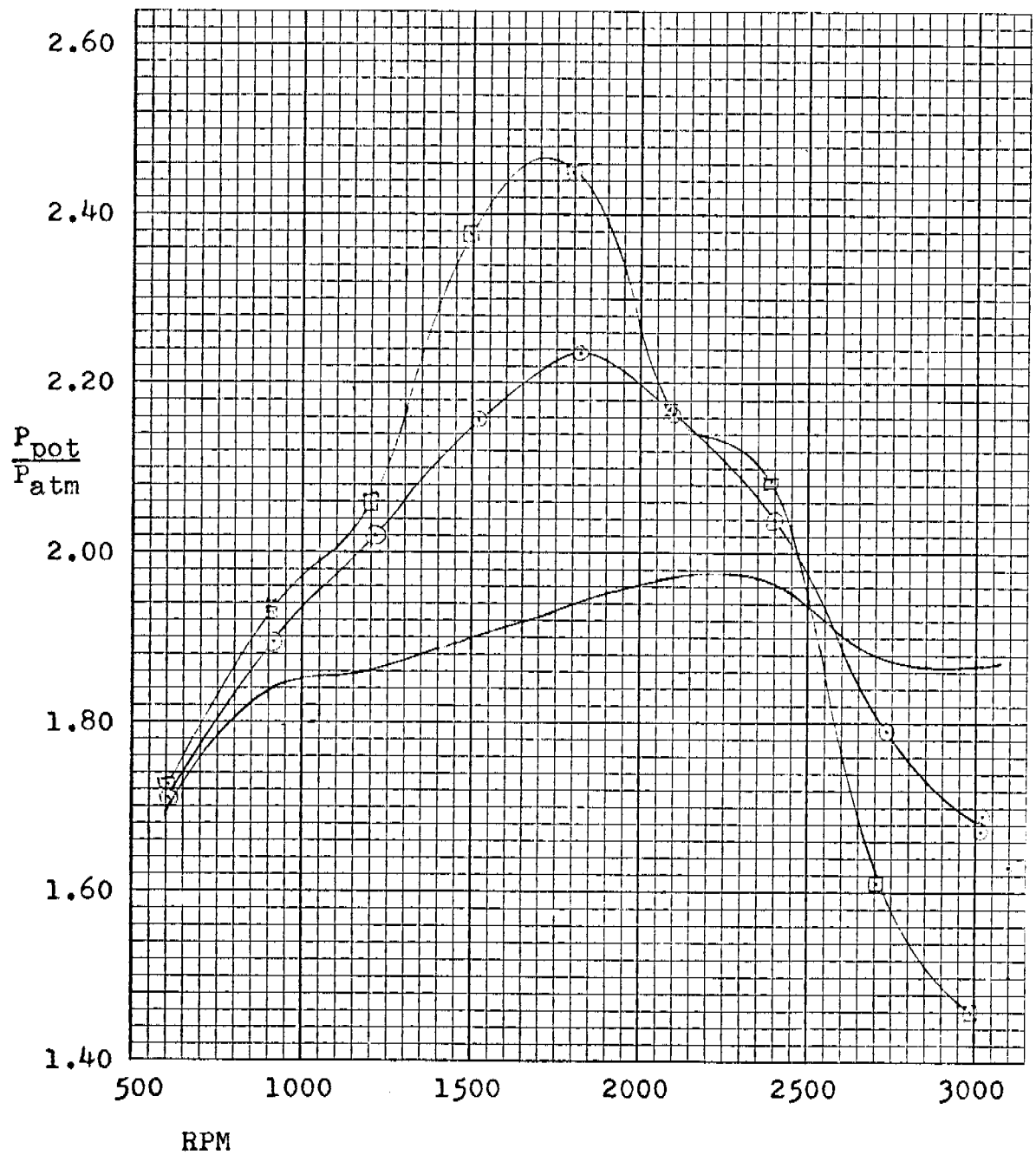


Figure 15

1½ pipe

cyl #	length
1	□ 25.1
2	○ 24.1, no nozzle
— Stock Manifold	

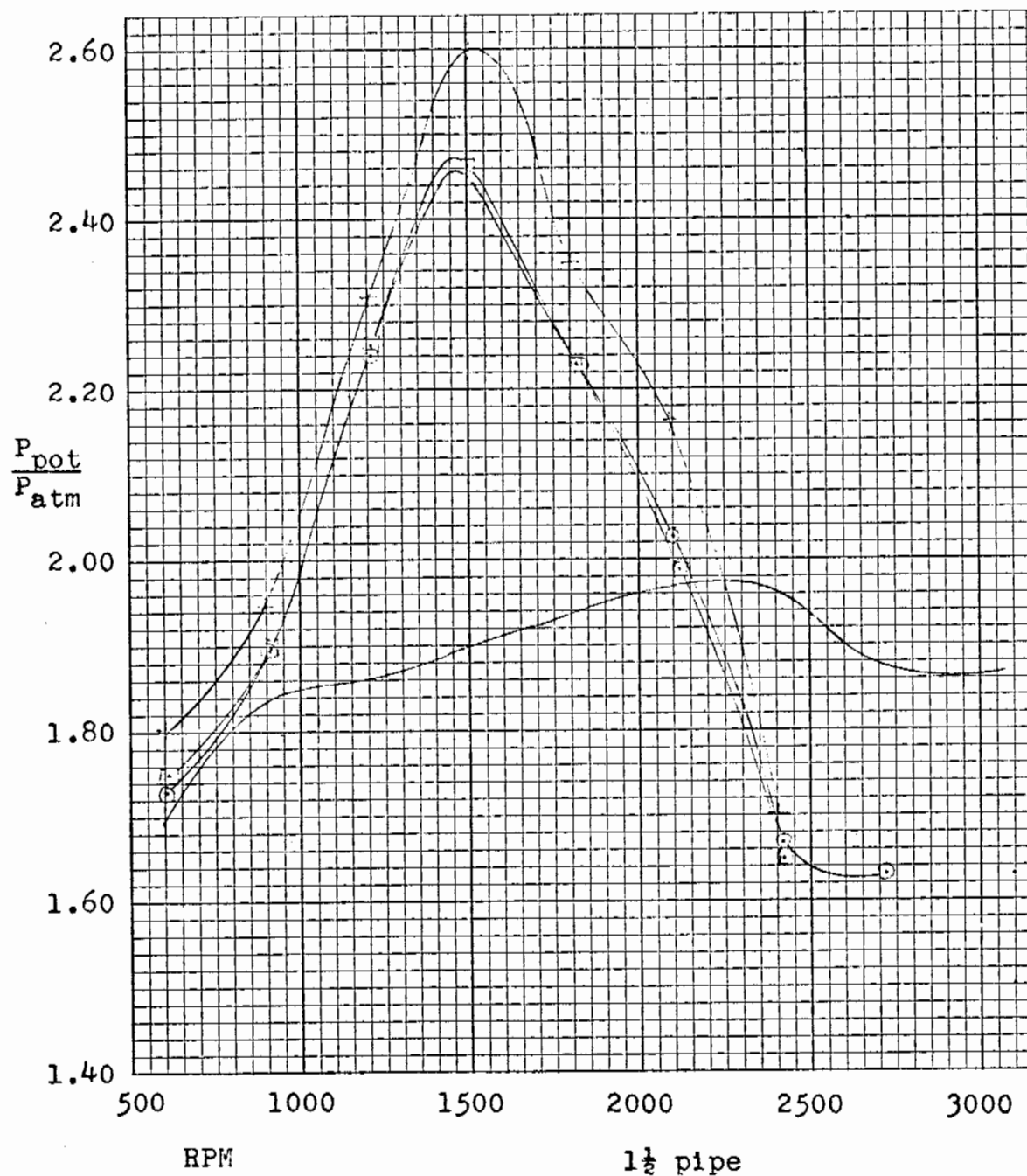


Figure 16

$1\frac{1}{2}$ pipe
 cyl # length
 2 + 45.0
 2 □ 44.1, 27" to bend
 2 ○ 44.1, 7" to bend
 — Stock Manifold

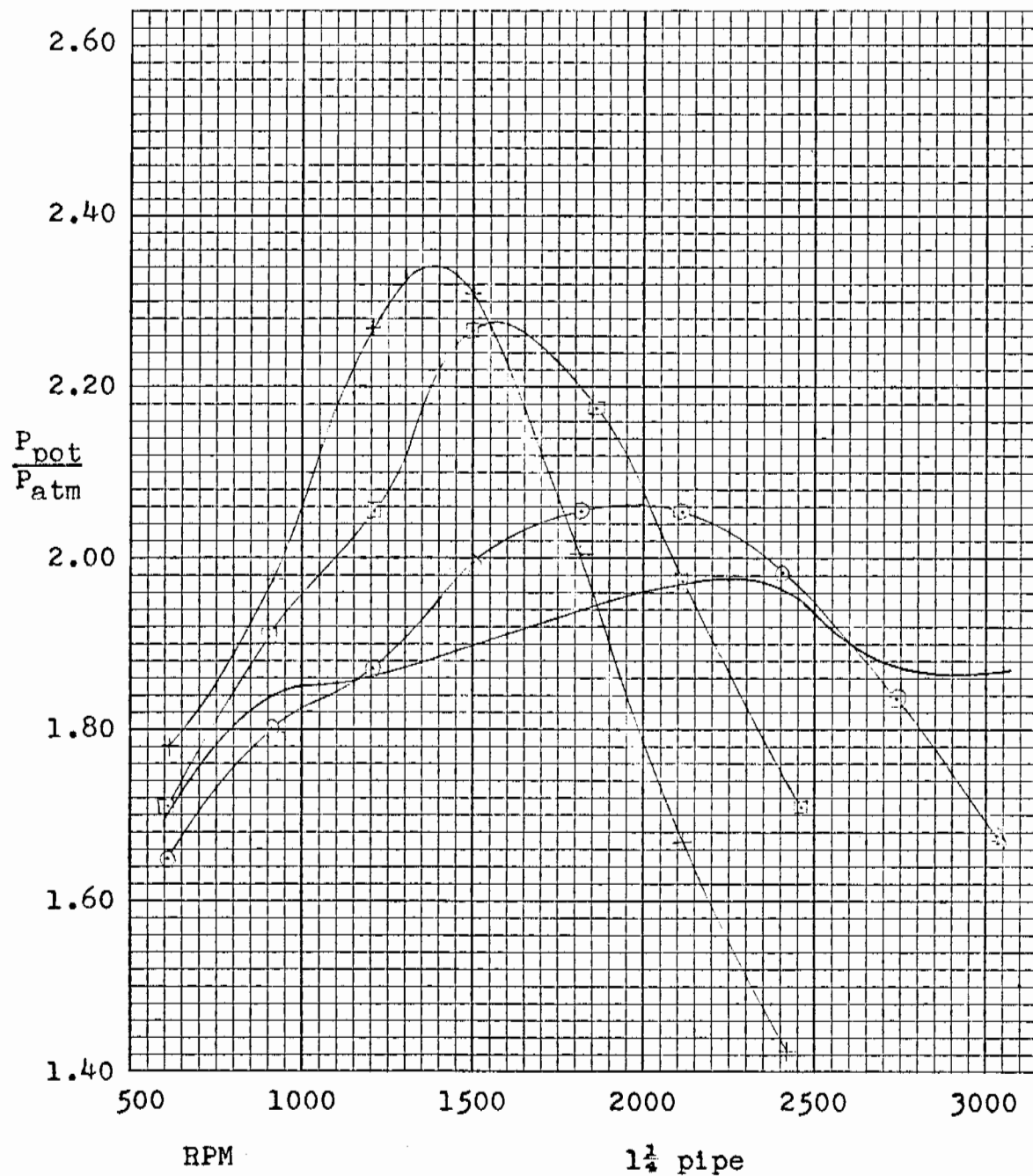


Figure 17

1 1/4 pipe
cyl # length

1 + 41.0

1 □ 26.9

1 ○ 10.0

— Stock Manifold

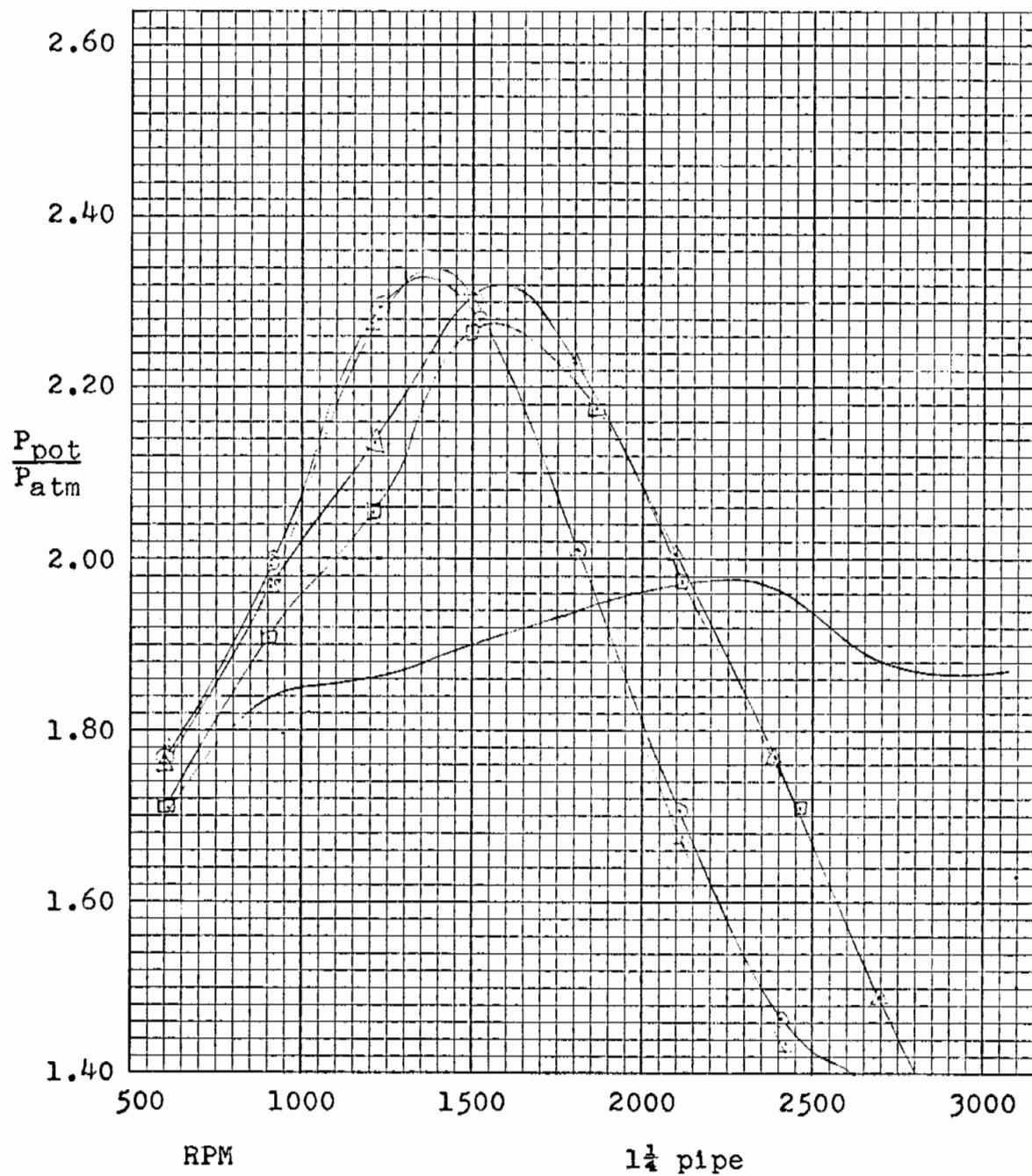


Figure 18

cyl #	length
1	⊙ 41.4, 11" to bend
1	+ 41.0
1	△ 27.5, 11" to bend
1	□ 26.9
— Stock Manifold	

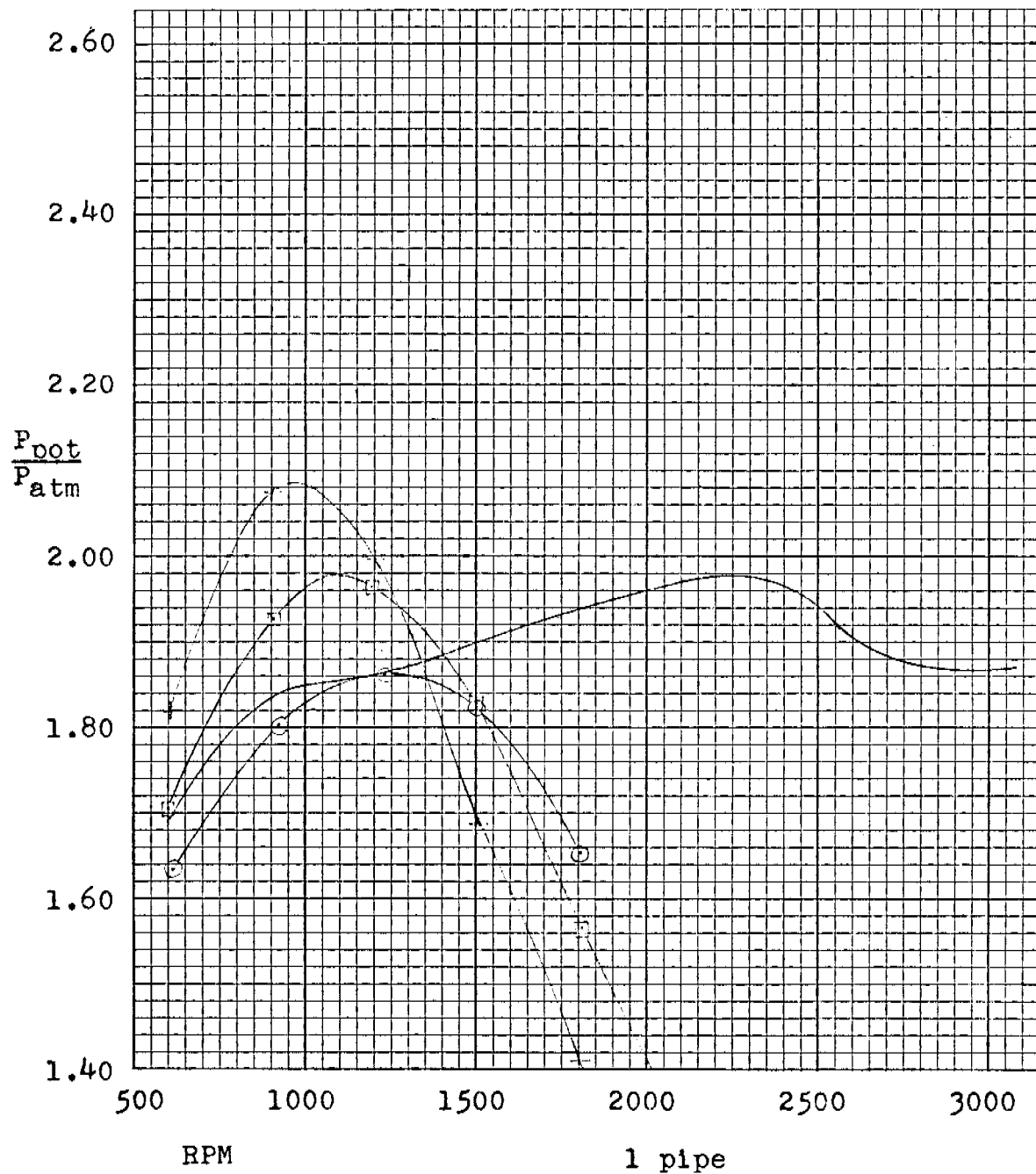


Figure 19

cyl # length

1 + 31.0

1 □ 16.8

1 ⊙ 8.7

— Stock Manifold

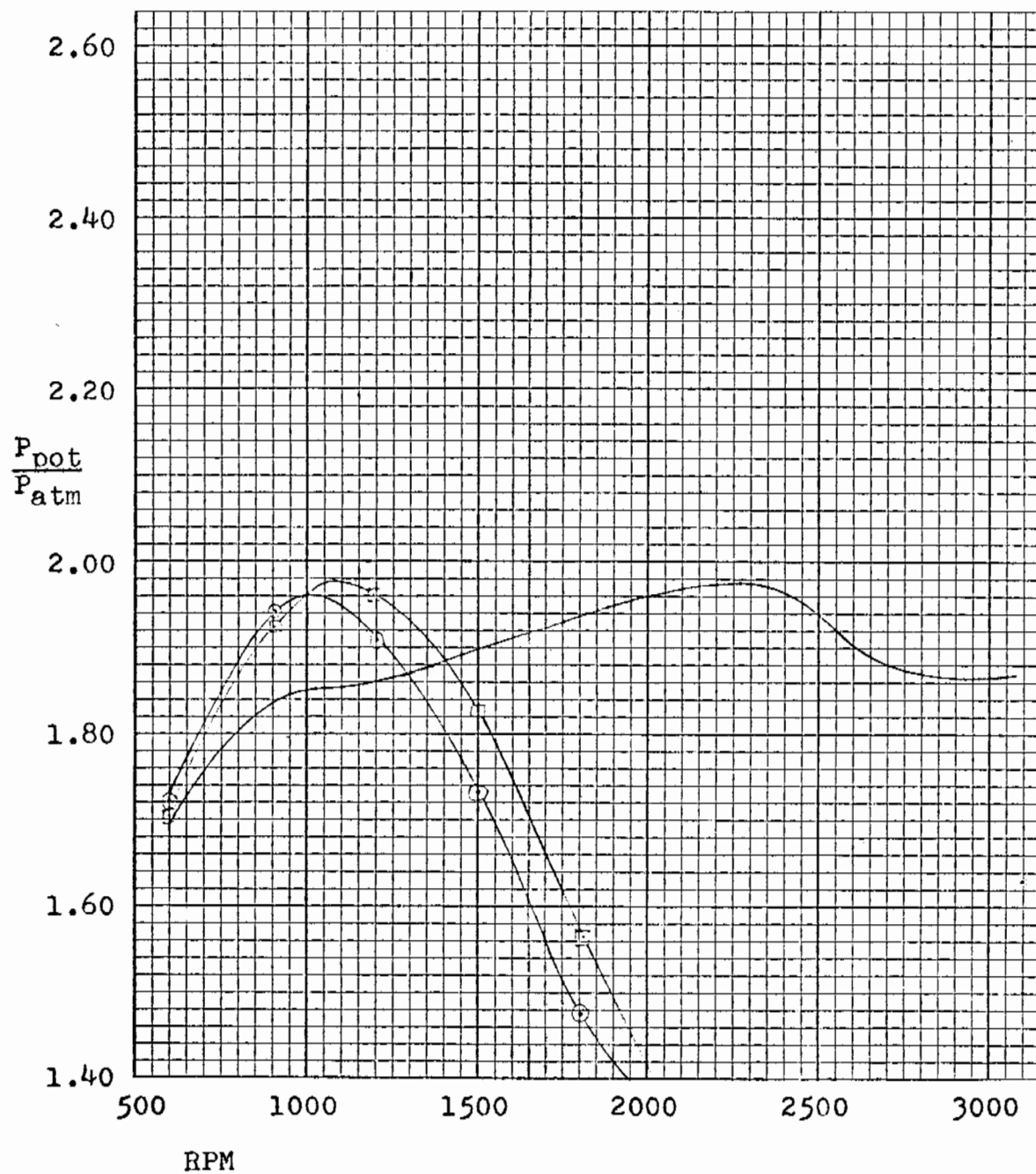


Figure 20

1 pipe
 cyl # length
 1 □ 16.8
 1 ○ 15.8, no nozzle
 — Stock Manifold

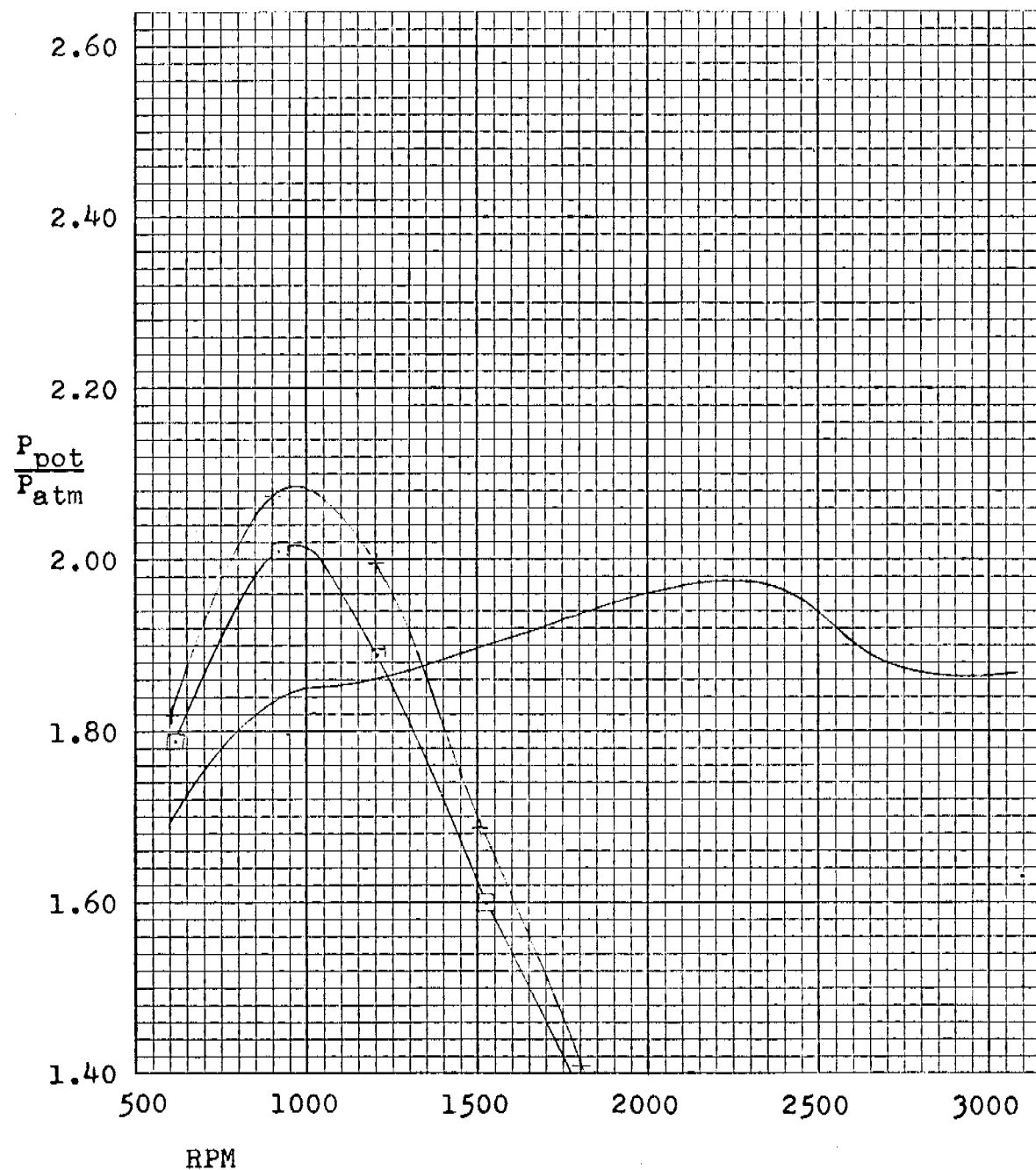


Figure 21

1 pipe
 cyl # length
 1 □ 32.0, 10" to bend
 1 + 31.0
 — Stock Manifold

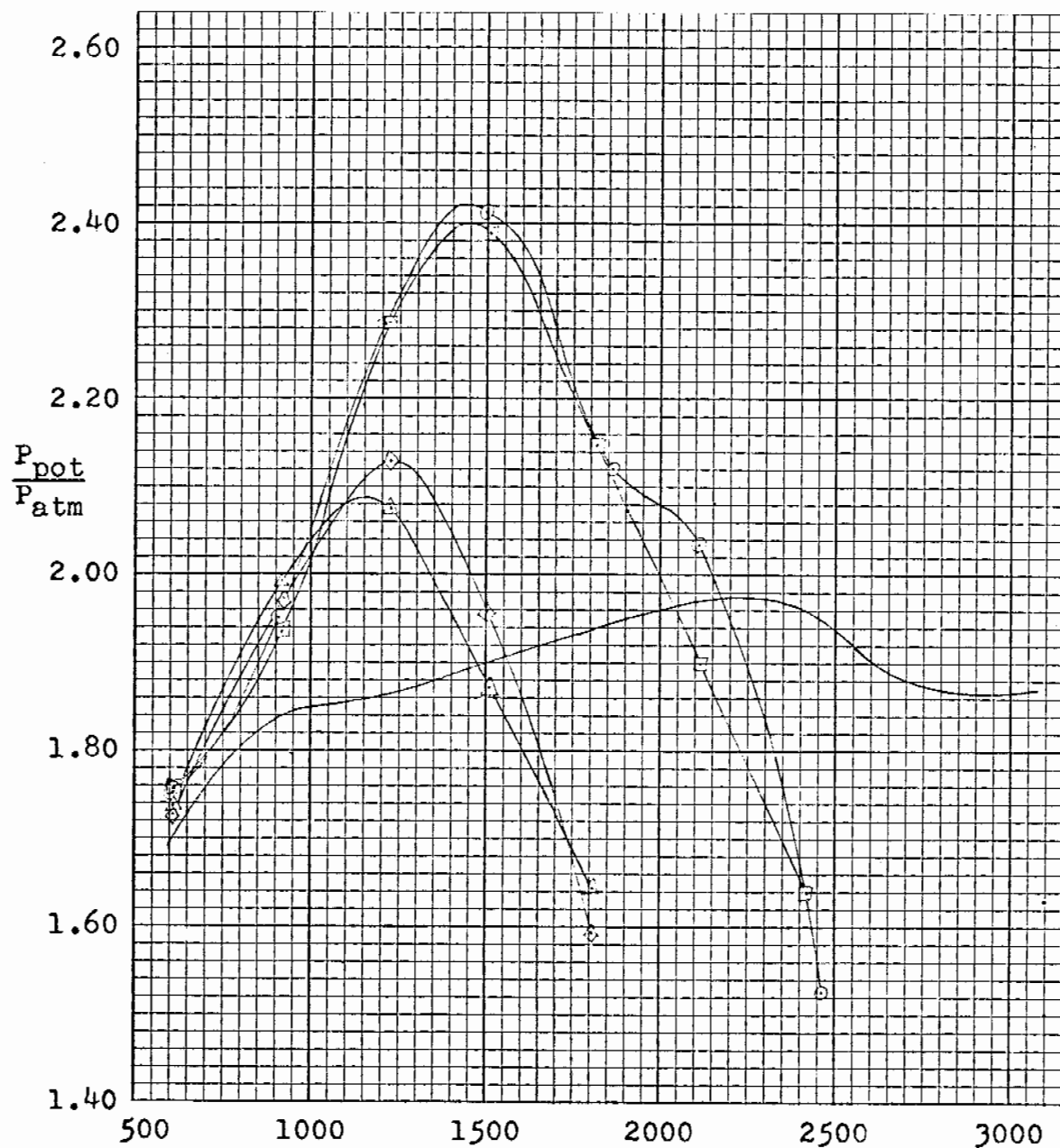


Figure 22

	cyl #	$1\frac{1}{2}$	$1\frac{1}{4}$	$1\frac{1}{2}$
2	⊙	4.4	14.4	21.2
2	⊠	24.3	15.2	
		$1\frac{1}{2}$	1	$1\frac{1}{2}$
2	◇	4.7	9.1	21.6
2	△	24.7	9.6	

— Stock Manifold

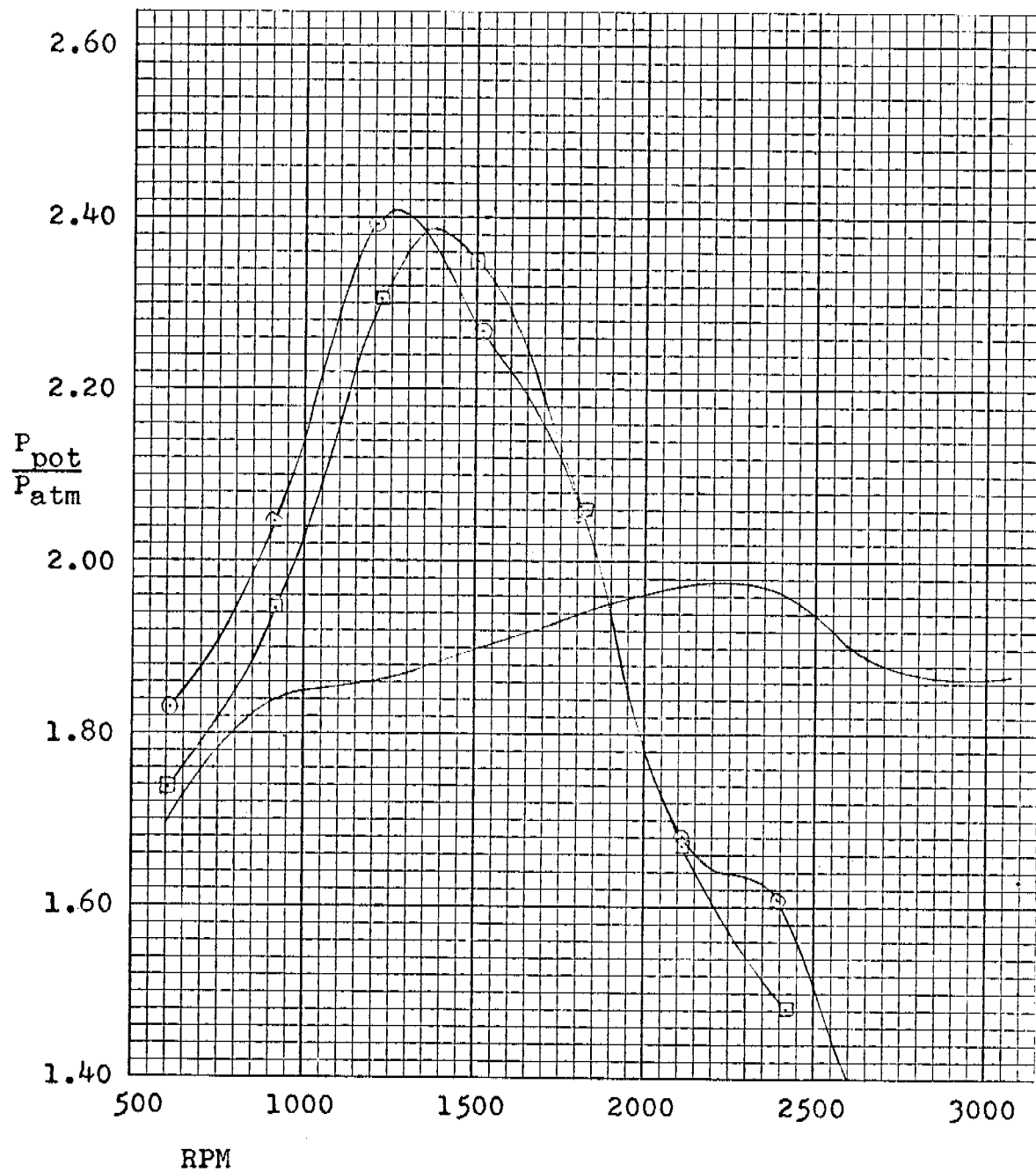


Figure 23

cyl #	$1\frac{1}{4}$	$1\frac{1}{2}$	$1\frac{3}{4}$
1	⊙ 9.2	20.5	18.0
1	□ 26.2	21.3	
— Stock Manifold			

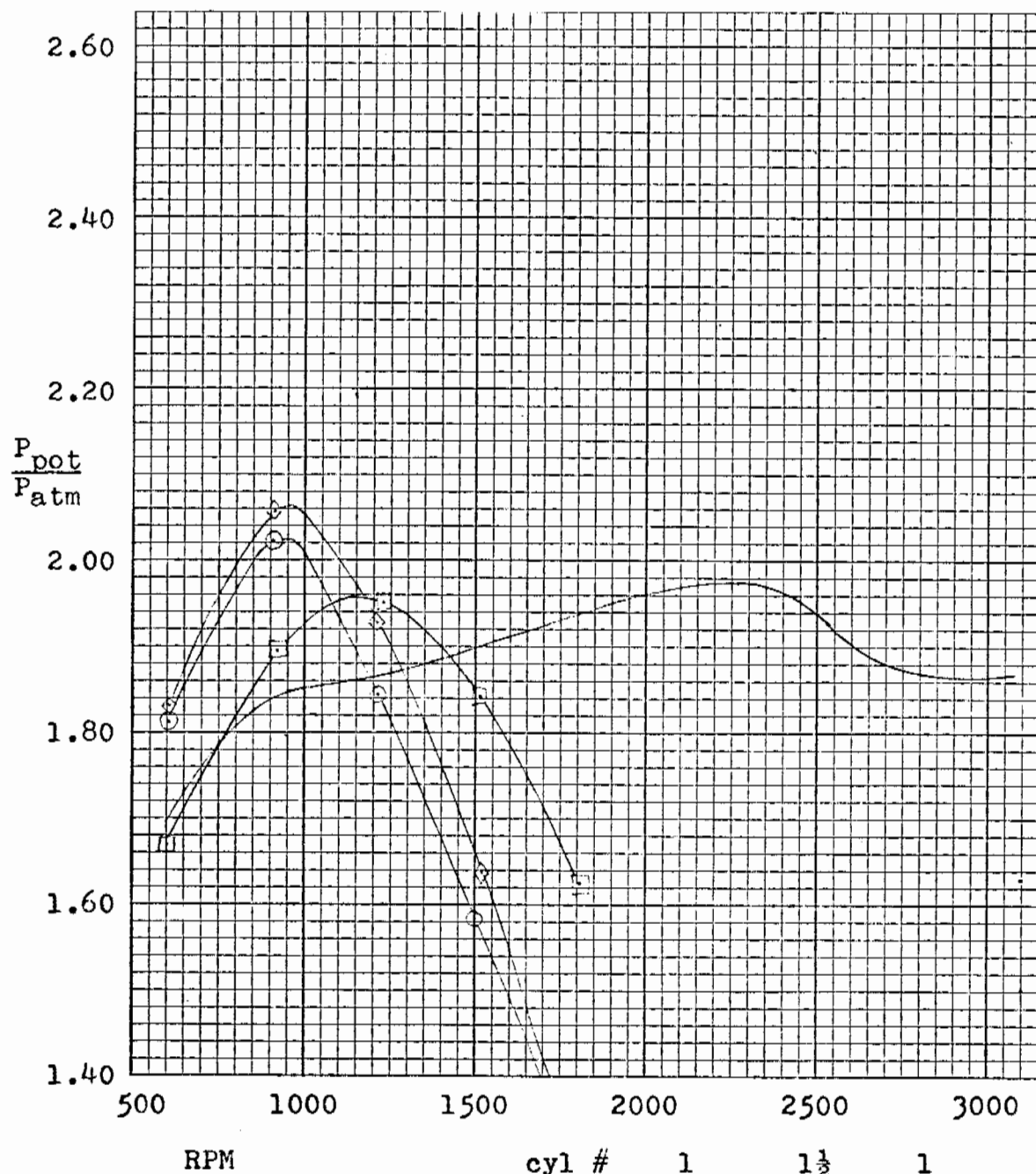


Figure 24

cyl #	1	1½	1	
1	⊙	8.3	21.2	15.7
1	⊠	8.3	21.6	
	1	1¼	1	
1	◊	8.0	14.6	15.5
— Stock Manifold				